

**PILOT STUDY OF NATURAL RADIOACTIVITY IN
VEGETABLES IN SELECTED LOCATIONS IN ONDO
STATE, NIGERIA.**

BY

**EYEBIOKIN, MOJISOLA RACHAEL
B. Tech (FUTA)
(PHY/95/6776)**

**A thesis submitted in the Department of Physics/Electronics to the
School of Postgraduate Studies in partial fulfillment of the
requirements for the degree of**

**MASTER OF TECHNOLOGY (HEALTH AND RADIATION PHYSICS)
FEDERAL UNIVERSITY OF TECHNOLOGY, AKURE**

SEPTEMBER, 2005.

CERTIFICATION

I certify that M.R Eyebiokin (PHY/95/6776) has carried out this work under my supervision in the Department of Physics/Electronics, Federal University of Technology, Akure, Ondo State. To the best of my knowledge the work has not been submitted elsewhere for the award of any degree or diploma of this, or any other, University.



.....
Dr A.B. Rabi B.Sc. (Horn), M.Sc., Ph.D. (Nigeria)
Supervisor

DEDICATION

This work is dedicated to Loving Mother Mrs. S. A. Eyebiokin and Loving Husband Mr. Oladipo Usikalu.

ACKNOWLEDGEMENTS

I give praise to God for his mercy, love and protection throughout the period of this work.

I am really grateful to my supervisor, Dr. A.B Rabiou for his interest in the work and for his constructive criticism and encouragement during the course of this work.

I appreciate the immense contributions of Dr A.M Arogunjo and Dr G. Oboh they suggested I carried out this work and provided some literature materials used in this work. I quite appreciate their generosity.

I will not fail to acknowledge the assistance both in cash and kind of Dr. F. Balogun, Mr. Tchokossa and Pastor Titilola of National Centre for Energy Research and Development (N.C.E.R.D.), Obafemi Awolowo University, Ile Ife, where the measurement reported in this work was carried out.

I am grateful to Professor (Mrs.) I. A. Fuwape, Dr M.O. Ajewole, Dr M.T Babalola, Dr O.S Ajayi and Mr. K.D Adedayo for their words of encouragement and fatherly advice. My sincere appreciations go to entire staff of Physics/Electronics Department, FUTA.

I am very grateful to my loving mother and my elder brothers for their care and for funding my course. I also thank my daddies, brothers, and sisters for their love and prayers.

Finally, my sincere thanks go to my husband Mr. Oladipo Usikalu for his understanding and assistance throughout the course of the work. Thank you all.

Eyebiokin, M. R.

September, 2005.

ABSTRACT

The activity concentrations of ^{40}K , ^{238}U and ^{232}Th in some vegetables commonly consumed in Jegele, Idanre and Agbabu have been measured using the gamma ray spectrometer consisting of a lead shielded 76mm by 76mm NaI (TI) detector crystal coupled to a Canberra series 10 plus multichannel analyzer. Preset counting time of 10 hours (36,000s) was used for each sample. Results showed that the concentrations of radionuclides varied from one location to another. The highest radioactivity concentration of 2459.73Bqkg^{-1} , 97.57Bqkg^{-1} and 18.44Bqkg^{-1} ^{40}K , ^{238}U and ^{232}Th , respectively was obtained from *Tatum Triangulare*, *Tatum Triangulare* and *African Spinach* respectively all in Idanre. The lowest concentration of 721.86Bqkg^{-1} , 2.36Bqkg^{-1} and 6.23Bqkg^{-1} ^{40}K , ^{238}U and ^{232}Th respectively was obtained from *Telfairia Occidentalis*, *Solanium Macncarpon* and *Corchorous Olitorious* in Jegele and Agbabu. The equivalent dose rates due to intake of the vegetables were determined. The mean effective dose equivalent for Jegele, Idanre and Agbabu were 0.59mSvyr^{-1} , 0.73mSvyr^{-1} and 0.64mSvyr^{-1} . These translate to collective doses of $2.95 \times 10^2 \text{manSvyr}^{-1}$, $1.46 \times 10^1 \text{manSvyr}^{-1}$ and $1.28 \times 10^1 \text{manSvyr}^{-1}$ for Jegele, Idanre and Agbabu respectively. All these values are lower than the recommended 2.4mSvyr^{-1} (UNCEAR, 1993) for normal background. The results presented here serve as reference for future radioactivity monitoring especially in Agbabu after the scheduled exploitation of the bitumen

TABLE OF CONTENTS

| | |
|-------------------|------|
| Title page | i |
| Certification | ii |
| Dedication | iii |
| Acknowledgement | iv |
| Abstract | v |
| Table of Contents | vi |
| List of Figures | vii |
| List of Tables | viii |

CHAPTER ONE: INTRODUCTION

| | | |
|-----|------------------------------------|---|
| 1.0 | Introduction | 1 |
| 1.1 | Specific Objective of the Research | 1 |
| 1.2 | Energy Sources and Radionuclides | 1 |
| 1.3 | The Scope of the Study | 2 |
| 1.4 | Geology of the Locations | 2 |

CHAPTER TWO: LITERATURE REVIEW

| | | |
|-----|---|----|
| 2.1 | Radioactivity | 5 |
| 2.2 | The Kinetics of Radioactive Decay Process | 5 |
| 2.3 | Half Life of Radioactive Elements | 6 |
| 2.4 | Radioactive Equilibrium | 6 |
| 2.6 | Radiation | 7 |
| 2.7 | Common Types of Radiation | 8 |
| 2.8 | Radionuclides | 12 |

| | | |
|--------|---|----|
| 2.8.1 | Primordial Radionuclides | 12 |
| 2.8.2 | Cosmogenic | 15 |
| 2.3.3 | Artificial Radionuclides | 19 |
| 2.9 | Review of Radiation Monitoring | 21 |
| 2.10 | Effects of Ionizing Radiation on Human Tissue | 22 |
| 2.10.1 | Acute Dose | 24 |
| 2.10.2 | Chronic Dose | 25 |

CHAPTER THREE

| | | |
|-------|-------------------------------------|----|
| 3.1 | Radiation Detection and Measurement | 26 |
| 3.1.1 | Photoelectric Absorption | 26 |
| 3.1.2 | Compton Scattering | 27 |
| 3.1.3 | Pair Production | 28 |
| 3.2 | Scintillation Detection | 29 |
| 3.2.1 | Scintillation Detection by NaI (Tl) | 30 |
| 3.2.2 | Photomultiplier Tube | 32 |
| 3.2.3 | Pulse shaping and Height Analysis | 34 |
| 3.3 | Resolution | 36 |
| 3.4 | Net Area Calculation | 38 |
| 3.4.1 | End -Point Averaging | 40 |
| 3.5 | Gamma- ray Spectrometry | 41 |



CHAPTER FOUR: MATERIALS AND METHOD

| | | |
|-------|-----------------------------------|----|
| 4.1 | Calibration | 42 |
| 4.1.1 | Energy Calibration | 42 |
| 4.1.2 | Efficiency Calibration | 46 |
| 4.2 | Sample Collection and Preparation | 49 |

| | | |
|--|--|----|
| 4.3 | Radioactivity Counting | 51 |
| CHAPTER FIVE: RESULT AND DISCUSSION | | |
| 5.1 | Activity Concentrations | 52 |
| 5.1.1 | Location 1 | 52 |
| 5.1.2 | Location 2 | 56 |
| 5.1.3 | Location 3 | 59 |
| 5.2 | Relative Variation of Radionuclides Concentration across the Species | 62 |
| 5.3 | Spatial Distribution of Radionuclides in the Window of Study | 63 |
| 5.4 | Effective Dose Equivalent and Collective Effective Dose equivalent | 67 |
| 5.5 | Conclusion | 72 |
| 5.6 | Limitations and Suggestion for Further Studies | 73 |
| | References | 74 |

LIST OF FIGURES

| | | |
|-----|---|----|
| 1.1 | Map showing the study areas (Adeniyi, 1998) | 4 |
| 3.1 | Schematic representation of the sequence of events in the detection of Gamma ray photon by a scintillation detection system | 31 |
| 3.2 | Photomultiplier tube | 33 |
| 3.3 | A schematic representation of a pulse shaping circuit | 35 |
| 3.4 | The gamma spectra of the primordial radionuclides | 37 |
| 3.5 | Net area determination | 39 |
| 4.1 | Schematic diagram of the measuring assembly | 43 |
| 4.2 | Graph showing energy channel dependence | 44 |
| 4.3 | The efficiency of the system as a function gamma energy | 48 |
| 5.1 | Mean radioactivity concentrations of ^{40}K , ^{238}U and ^{232}Th in location 1 | 54 |
| 5.2 | Mean radioactivity concentrations of ^{40}K , ^{238}U and ^{232}Th in location 2 | 57 |
| 5.3 | Mean radioactivity concentrations of ^{40}K , ^{238}U and ^{232}Th in location 3 | 60 |
| 5.4 | Spatial Distribution of the ^{40}K across the Three Stations | 64 |
| 5.5 | Spatial Distribution of the ^{238}U across the Three Stations | 65 |
| 5.6 | Spatial Distribution of the ^{232}Th across the Three Stations | 66 |

LIST OF TABLES

| | | |
|-----|--|----|
| 2.1 | Lists of primordial radionuclides | 14 |
| 2.2 | Calculated cosmic ray doses | 16 |
| 2.3 | Cosmogenic nuclides | 18 |
| 2.4 | Human produced nuclides | 20 |
| 4.1 | Energy channel linear relationship | 45 |
| 4.2 | Detector efficiencies at different γ energy | 47 |
| 4.3 | Vegetables investigated in Jegele with their botanical names | 50 |
| 4.4 | Vegetables investigated in Idanre with their botanical names | 50 |
| 4.5 | Vegetables investigated in Agbabu with their botanical names | 51 |
| 5.1 | Mean radioactivity concentrations of the radionuclides in location 1 | 55 |
| 5.2 | Mean radioactivity concentrations of the radionuclides in location 2 | 58 |
| 5.3 | Mean radioactivity concentrations of the radionuclides in location 3 | 61 |
| 5.4 | Effective dose equivalent in location 1 vegetables | 69 |
| 5.5 | Effective dose equivalent in location 2 vegetables | 69 |
| 5.6 | Effective dose equivalent in location 3 vegetables | 70 |
| 5.7 | Dose limits and their biological effects | 71 |

exploration cannot be preempted. Hence the inclusion of bitumen producing area in this research.

1.3 THE SCOPE OF THE STUDY

The primary aim of the present research is to investigate the radioactivity levels in the edible parts of locally grown vegetables in a bitumen producing area specifically Agbabu, compare the activity level with the same vegetables obtained from Idanre a rocky town and 'Akure with normal vegetation to serve as control. This will be done with γ spectrometer using NaI (TI) detector coupled through a pre-amplifier base to a multichannel analyzer (MCA) in the Centre for Energy Research and Development Obafemi Awolowo University, Ile-Ife. Attempt was made to determine the absorbed radiation dose and the equivalent radiation dose to the people in the areas consuming these vegetables.

1.4 GEOLOGY OF THE LOCATIONS

Jegele (7°N , 5°E) is under the jurisdiction of Akure North local Government which was created in 1997 from Akure local Government(Omole, 2001). It is below 300m, dissected by innumerable streams and rivers flowing in broad sandy valleys. It lies mainly in the basins of the major rivers and fall roughly within the areas of sedimentation (www.ondostategovernment.com)

Idanre (9°N , 7°E) is under Idanre local Government the land is dominated igneous structures that form most of highlands and hills. The rocks of the basement complex, mainly of igneous origin, are encountered in over 60% of the surface area. Most of the area lies between 300 to 600m however the Idanre hills ,where the plateau is highest are about 1000m above the sea level (www.ondostategovernment.com)

Agbabu (6⁰N, 4⁰E) the rocks in this area are made of sandstones, shale, clays and coal. It lies adjacent to the seas. It runs along the coast from east to west in a strip of land and are made up of recent deposits of sand, clays and mud. Sands predominate and sand-bars cut off east-west lagoons. It consists mainly of muddy deposits pushed out by the Niger into a relatively tideless salt sea. The creeks and water channels form important fishing grounds and provide highways in this marshy area. It consists mostly of medium to fine grained sand stones interbedded with relatively thick siltstones and shale. The shale are rich in organic matter. They are brackish water shales below but become marine towards the top with abundant of fossils (www.fao.org/WAICENT/FAOINFO). Figure 1.1 shows the map of the study areas.



Fig. 1.1 Map showing the study areas (Adeniyi, 998).

CHAPTER TWO

LITERATURE REVIEW

2.1 RADIOACTIVITY

In 1896, Becquerel, who was investigating the relationship between X-rays and fluorescence using crystal of uranium potassium sulphate accidentally discovered that uranium compounds emit radiation that are similar to X-rays. Later, Pierre and Marie Curie, during their investigation of naturally occurring uranium ores, also discovered that radium (Ra), thorium (Th), and polonium (Po) are radioactive as well. Presently, over 60 radioactive elements can be found in nature and are grouped into primordial, cosmogenic and human produced.

2.2 THE KINETICS OF RADIOACTIVE DECAY PROCESS

The radioactivity of a sample of radioactive material is an important quantity or property of the sample. Activity itself is the rate at which the nuclei within the sample undergo transitions and can be expressed in terms of number of transitions per second (tps) or disintegration per second (dps). The Becquerel is the S.I unit, and is equivalent to 1 tps.

The probability that a nucleus will decay in a certain time interval does not depend on age of the nuclear, state of the chemical combination, temperature, pressure or presence of other atoms or nuclei, but a property of individual isolated nucleus. Therefore, the rate of decay from a sample of any radioactive substance must be proportional only to the number of nuclei present (Sprawls, 1995).

In a sample containing N nuclei, the rate of decay dN/dt will be

$$\frac{dN}{dt} = -\lambda N \quad 2.1$$



Where N is the number of atom present at time t , and λ is the decay constant with the characteristic value of the nuclei under consideration

Integrating equation (1.1)

$$\text{Therefore } N = N_0 e^{-\lambda t} \quad 2.2$$

This shows that the number of nuclei remaining decreases exponentially with time.

2.3 HALF LIFE OF RADIOACTIVE ELEMENTS

A fundamental characteristic of radioactivity is that all nuclei even of the same radioactive nuclide do not have the same lifetime. It is difficult to know the lifetime of a particular nuclide, but the average life time, which is a unique characteristic of each nuclide can be known. The average lifetime is expressed as the half-life ($T_{1/2}$), which is the time required for half of the initial number no of the nuclei to decay (sprawls, 1995).

From equation (2.1)

$$N = N_0 e^{-\lambda t}$$

$$t_{1/2} = \frac{0.693}{\lambda} \quad 2.3$$

2.4 RADIOACTIVE EQUILIBRIUM

When the presence and amount of the parent radionuclide of a particular decay series is to be determined by the measurement of the radioactivity of any of its daughter element, as is done in Gamma ray spectrometer, radioactive equilibrium becomes an important subject for consideration.

Gamma ray spectrometer can be used to determine the concentration of U, Th and K in a rock or soil sample because gamma rays of specific energy are associated with each radioelement. Energy of peaks in an energy spectrum of gamma ray being emitted by a radionuclide could be used to infer the particular radionuclide. The method involves the

county of gamma ray photon with specified energies, particularly those emitted by daughter product e.g. Bi – 234 in U – 238 decay series and Tl-208 in the 232 decay series. The gamma ray count rate can then be related to the amount of present by assuming there is a direct relation between the amount of daughter and parent. This assumption is only valid when the radioactive decay series is in a state of secular equilibrium.

When a radioactive element in a series is being formed, and at the same time transiting, if the parent nuclide forming the radio element under consideration has a considerably longer half life, that is long enough that there is a no noticeable decay during time interval of interest, a condition of secular equilibrium results. A radioactive series is said to be in a state of secular equilibrium when the number of atom of each daughter being produced in a series is equal to the number of atom of each daughter being produced in a series is equal to the number of atoms of that daughter being lost by decay. At such time, In a radioactive series in which the parent radionuclide have a considerably long half-life as stated above and the daughter nuclides are decaying into one another, at a point in time, the amount of any given daughter radionuclide will be constant.

At such time, it is possible to determine the amount of the parent of the decay series by measuring the radioactivity from any daughter nuclide (sprawls, 1995)

2.6 Radiation

According to the National Council on Radiation Protection and Measurement (NCRPM, 1987), humans have been exposed to radiation from natural sources since the dawn of time. The sources include the ground we walk on, the air we breathe, the food we eat and the solar system as a whole. Everything in our world contains small amounts of radioactive elements like Potassium 40, Radium 226 and Radon 222. These are either left

over from the creation of the world (like Uranium and Radium) or made by interactions with cosmic radiation (like Carbon 14 and Tritium). The Earth is constantly in a flux of cosmic radiation from outer space.

2.7 Common Types of Radiation

Sources of Ionizing Radiation with matter

As ionizing radiation moves from point to point in matter, it loses its energy through various interactions with the atoms it encounters. The rate at which this energy loss occurs depends upon the type and energy of the radiation and the density and atomic composition of the matter through which it is passing.

The various types of ionizing radiation impart their energy to matter primarily through excitation and ionization of orbital electrons. The term excitation is used to describe an interaction where electrons acquire energy from a passing charged particle but are not removed completely from their atom. Excited electrons may subsequently emit energy in the form of x-rays during the process of returning to a lower energy state. The term ionization refers to the complete removal of an electron from an atom following the transfer of energy from a passing charged particle. In describing the intensity of ionization, the term specific ionization is often used. This is defined as the number of ion pairs formed per unit path length for a given type of radiation

Gamma-rays

A nucleus which is in an excited state may emit one or more photons (packets of electromagnetic radiation) of discrete energies. The emission of gamma rays does not alter the number of protons or neutrons in the nucleus, but instead has the effect of moving the nucleus from a higher to a lower energy state (unstable to stable). Gamma ray emission frequently follows beta decay, alpha decay, and other nuclear decay processes.

Beta (β) Particles

A nucleus with an unstable ratio of neutrons to protons may decay through the emission of a high speed electron called a beta particle. This results in a net change of one unit of atomic number (Z). Beta particles, these are electrons, with a charge of -1 . They are emitted when a neutron splits into a proton and electron (β^-), ($n \rightarrow P + \beta^- + \nu$). The proton stays in the nucleus, while the electron is ejected in radioactive disintegration. The emission is as represented below.



Where Z = number of protons

A = mass number

A positron (β^+) can also be produced by splitting of a proton

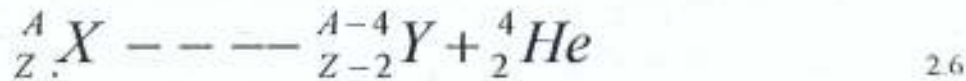


The result of the transmutation is that there will be a gain in atomic number with no change in mass, as expressed above.

The β^- particles are capable of traveling at great speed, therefore they have a greater penetrating power above 100 times that of α^- particles. They can be stopped by some millimeters thick aluminum foil. Their low masses allow them to be deflected to a large extent in an electric or magnetic field in the opposite direction to that of alpha particles. Beta particles have a negative charge and the beta particles emitted by a specific radionuclide will range in energy from near zero up to a maximum value, which is characteristic of the particular transformation.

Alpha (α) Particles

Certain radionuclides of high atomic mass (^{226}Ra , ^{238}U , ^{239}Pu) decay by the emission of alpha particles. These alpha particles are tightly bound units of two neutrons and two protons each (^4He nucleus) and have a positive charge. Their penetrating power is very low, being stoppable by a sheet of aluminum or paper. Their emission during disintegration may be expressed as follows:



Where,

Z = number of protons

N = number of neutrons

From the expression above, it is obvious that an alpha particle emission result in the transition of an initial element X to a new element Y . Emission of an alpha particle from the nucleus results in a decrease of two units of atomic number (Z) and four units of mass number (A). Alpha particles are emitted with discrete energies characteristic of the particular transformation from which they originate. All alpha particles from a particular radionuclide transformation will have identical energies.

Neutrons

Neutrons are neutral particles that are normally contained in the nucleus of all atoms and may be removed by various interactions or processes like collision and fission. Neutrons are typically produced by one of three methods. Large amounts of neutrons are produced in nuclear reactors due to the nuclear fission process. High energy neutrons are also produced by accelerating deuterons that causes them to interact with tritium nuclei. The third method of producing neutrons is by bombarding beryllium with alpha particles. Neutron sources can be made using the alpha-neutron reaction on beryllium by making a

mixture of powered alpha emitter and beryllium and sealing it in a metal container. Early neutron sources used radium as the alpha emitter. Modern neutron sources typically use plutonium or americium as the alpha source. The radium-beryllium (Ra-Be) sources were also sources of large amounts of gamma radiation while the plutonium-beryllium (Pu-Be) sources and the americium-beryllium (Am-Be) sources only produce small amounts of very low energy gamma radiation. Thus, as neutron sources, Pu-Be and Am-Be sources tend to be less hazardous to handle. The older Ra-Be sources also had a tendency to develop leaks over time and give off radon gas, one of the products of radium decay.

X rays

X-rays are electromagnetic waves or photons not emitted from the nucleus, but normally emitted by energy changes in electrons. These energy changes are either in electron orbital shells that surround an atom or in the process of slowing down such as in an X-ray machine. X-rays are distinguished from gamma rays only by their source (orbital electrons rather than the nucleus). X-rays are emitted with discrete energies by electrons as they shift orbits following certain types of nuclear decay processes. Internal conversion occurs in a isotope when the energy is transferred to an atomic origin electron that is then ejected with kinetic energy equal to the expected gamma ray, but minus the electron's binding energy. The vacancy in the atomic structure is filled by an external electron, resulting in the production of x-rays. Thulium-170 is a good example of this type of disintegration. When Thulium-170 loses its energy it will exhibit a 60 % probability of interaction with an orbital electron thus producing x-radiation.

2.8 Radionuclides

Our world is radioactive and has been since it was created. Over 60 radionuclides (radioactive elements) can be found in nature, and they can be placed in three general categories:

1. Primordial - from before the creation of the Earth
2. Cosmogenic - formed as a result of cosmic ray interactions
3. Artificial Radionuclides - enhanced or formed due to human actions (minor amounts compared to natural) Radionuclides are found naturally in air, water and soil. They are even found in us, being that we are products of our environment. Every day, we ingest and inhale radionuclides in our air and food and the water. Natural radioactivity is common in the rocks and soil that makes up our planet, in water and oceans, and in our building materials and homes. There is nowhere on Earth that you can not find natural radioactivity.

Radioactive elements are often called radioactive isotopes or radionuclides or just nuclides. There are over 1,500 different radioactive nuclides. Often, radionuclides are symbolized based on the element and on the atomic weight, as in the case of radioactive hydrogen or tritium with an atomic weight of 3 is shown as H-3 or ^3H . As another example, Uranium with the atomic weight of 235 would be shortened to U-235 or ^{235}U . (Taylor & Francis, 1991)

2.8.1 Primordial radionuclides

Primordial radionuclides are left over from when the world and the universe were created. They are typically long lived, with half-lives often of the order of hundreds of millions of years.

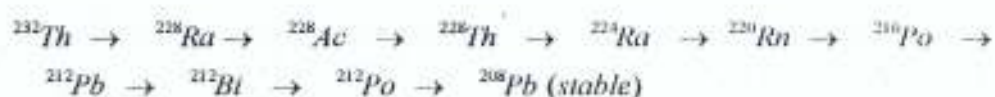
Radon comes from the decay of Uranium, a natural element. Uranium decays through a long chain of radionuclides that includes radon. Radon is a noble gas, not chemically active so it migrates through porous materials like the ground and foundation of buildings. Radon itself has a small chance of decay as it is breathed in and out. Most dose comes from the decay products of radon, sometimes called radon daughters or radon progeny. These radon progeny are particles not gases, and can be deposited in lungs as we breathe. There they have some chance of decaying before the body can get rid of them, resulting in a radioactive dose.

There are several other naturally occurring radioactive nuclides. Most notable are Carbon-14 (C-14) and Potassium-40 (K-40). They are made by cosmic ray interactions and eventually make their way into our food chain. Once ingested, they can decay and give us an internal dose. All living organic material has a constant ratio of carbon 14 to non-radioactive carbon 12. Once dead, the organic material stops taking in carbon. Therefore, by measuring that ratio of C-14 to C-12 found in organic archeological items, the appropriate time since death can be determined. This is what is known as carbon dating.

Table 2.1 Lists of Primordial Radionuclides (BIER V NAS)

| Primordial Nuclide | Symbol | Half-life | Natural Activity |
|--------------------|-------------------|--------------------------|--|
| Uranium 235 | ^{235}U | 7.04×10^8 yr | 0.72% of all natural uranium |
| Uranium 238 | ^{238}U | 4.47×10^9 yr | 99.2745% of all natural uranium; 0.5 to 4.7 ppm total uranium in the common rock types |
| Thorium 232 | ^{232}Th | 1.41×10^{10} yr | 1.6 to 20 ppm in the common rock types with a crustal average of 10.7 ppm |
| Radium 226 | ^{226}Ra | 1.60×10^3 yr | 0.42 pCi/g (16 Bq/kg) in limestone and 1.3 pCi/g (48 Bq/kg) in igneous rock |
| Radon 222 | ^{222}Rn | 3.82 days | Noble Gas, annual average air concentrations range in the US from 0.016 pCi/L (0.6 Bq/m ³) to 0.75 pCi/L (28 Bq/m ³) |
| Potassium 40 | ^{40}K | 1.28×10^9 yr | soil - 1-30 pCi/g (0.037-1.1 Bq/g) |

Some nuclides like ^{232}Th have several members of its decay chain.



Some other primordial radionuclides are ^{50}V , ^{87}Rb , ^{113}Cd , ^{115}In , ^{123}Te , ^{138}La , ^{142}Ce , ^{144}Nd , ^{147}Sm , ^{152}Gd , ^{174}Hf , ^{176}Lu , ^{187}Re , ^{190}Pt , ^{192}Pt , ^{209}Bi .

2.8.3 Cosmogenic

Cosmic radiation is really divided into two types, primary and secondary. Primary cosmic radiation is made up of extremely high energy particles (up to 10^{18} eV), and are mostly protons, with some larger particles. A large percentage of it comes from outside of our solar system and is found throughout space. Some of the primary cosmic radiation is from our sun, produced during solar flares.

Little of the primary cosmic radiation penetrates to the Earth's surface; the vast majority of it interacts with the atmosphere. When it does interact, it produces the secondary cosmic radiation, or what we actually see here on Earth. These reactions produce other lower energy radiations in the form of photons, electrons, neutrons and muons that make it to the surface.

The atmosphere and the Earth's magnetic fields also act as shields against cosmic radiation, reducing the amount that reaches the Earth's surface. Cosmic radiation depends on what altitude one is.

There is only about a 10% decrease at sea level in cosmic radiation rates when going from pole to the equator, but at 16975m the decrease is 75%. This is on account of the effect of the earth's and the Sun's geomagnetic fields on the primary cosmic radiations.

Flying can add a few extra mSv to annual dose, depending on how often one flies, how high the plane flies, and how long one stays in the air. Table 2.2 shows the variation of height with cosmic radiation absorbed.

Table 2.2 Calculated Cosmic Ray Doses (BIER V NAS)

| Calculated cosmic ray doses to a person flying in subsonic and supersonic aircraft under normal solar conditions | | | | |
|--|--------------------------|---------------------|----------------------------|---------------------|
| Route | Subsonic flight at 11 km | | Supersonic flight at 19 km | |
| | Flight duration (hrs) | Dose per round trip | Flight duration (hrs) | Dose per round trip |
| | | (μGy) | | (μGy) |
| Los Angeles-Paris | 11.1 | 48 | 3.8 | 37 |
| Chicago-Paris | 8.3 | 36 | 2.8 | 26 |
| New York-Paris | 7.4 | 31 | 2.6 | 24 |
| New York-London | 7.0 | 29 | 2.4 | 22 |
| Los Angeles-New York | 5.2 | 19 | 1.9 | 13 |
| Sydney-Acapulco | 17.4 | 44 | 6.2 | 21 |

The source being primarily outside of our solar system. The radiation is in many forms, from high speed heavy particles to high energy photons and muons. The upper atmosphere interacts with many of the cosmic radiations, and produces radioactive nuclides. They can have long half-lives, but the majority has shorter half-lives than the primordial nuclides. Some common cosmogenic nuclides are listed in Table 2.3.

Table 2.3 Cosmogenic Nuclides (BIER V NAS)

| Nuclide | Symbol | Half-life | Source | Natural Activity |
|-----------|-----------------|-----------|--|---|
| Carbon 14 | ^{14}C | 5730 yr | Cosmic-ray interactions, $^{14}\text{N}(n,p)^{14}\text{C}$; | 6 pCi/g (0.22 Bq/g) in organic material |
| Tritium | ^3H | 12.3 yr | Cosmic-ray interactions with N and O; spallation from cosmic-rays, $^6\text{Li}(n,\alpha)^3\text{H}$ | 0.032 pCi/kg (1.2×10^{-3} Bq/kg) |

Some other cosmogenic radionuclides are ^{10}Be , ^{26}Al , ^{36}Cl , ^{80}Kr , ^{14}C , ^{32}Si , ^{39}Ar , ^{22}Na , ^{35}S ,

^{37}Ar , ^{33}P , ^{32}P , ^{38}Mg , ^{24}Na , ^{38}S , ^{31}Si , ^{18}F , ^{39}Cl , ^{38}Cl , ^{34m}Cl

2.8.3 Artificial Radionuclides

Artificial radionuclides in the environment result from the atmospheric testing of nuclear weapons, the exploitation of nuclear fission for the production of electricity and, to a lesser extent, the Chernobyl accident. The study of these artificial radionuclides in the environment is of interest for a number of reasons: firstly, to gain an understanding of their geochemical behavior; secondly, to aid in the assessment of their radiological significance to both present and future generations and, finally, with a greater understanding of their behavior, these radionuclides can, in turn, be used as geochronological tracers in the study of natural processes. Which include

- Transuranic elements (Np, Pu, Am) in the environment.
- Geochemical associations of artificial radionuclides in saltmarsh deposits.
- Pollutant dispersion and concentration mechanisms in the Irish Sea.
- The use of ^{137}Cs as a tracer of water movement.
- The biogeochemical behavior of novel radioactive pollutants (e.g. ^{99}Tc).
- Anthropogenic ^{14}C in the aquatic and terrestrial environments.
- The application of aerial and vehicular gamma-ray survey methods to the determination of the distribution and movement of radionuclides in the environment.

Humans have used radioactivity for one hundred years, and through its use, added to the natural inventories. The amounts are small compared to the natural amounts discussed above, and due to the shorter half-lives of many of the nuclides, have seen a marked decrease since the halting of above ground testing of nuclear weapons. Examples of few human produced or enhanced nuclides are listed in Table 2.4

Table 2.4 Human Produced Nuclides (Knoll,1989)

| Nuclide | Symbol | Half-life | Source |
|---------------|-------------------|-----------------------|---|
| Tritium | ^3H | 12.3 yr | Produced from weapons testing and fission reactors; reprocessing facilities, nuclear weapons manufacturing |
| Iodine 131 | ^{131}I | 8.04 days | Fission product produced from weapons testing and fission reactors, used in medical treatment of thyroid problems |
| Iodine 129 | ^{129}I | 1.57×10^7 yr | Fission product produced from weapons testing and fission reactors |
| Cesium 137 | ^{137}Cs | 30.17 yr | Fission product produced from weapons testing and fission reactors |
| Strontium 90 | ^{90}Sr | 28.78 yr | Fission product produced from weapons testing and fission reactors |
| Technetium 99 | ^{99}Tc | 2.11×10^5 yr | Decay product of ^{99}Mo , used in medical diagnosis |

2.9 Review of Radiation Monitoring

The possible effects of exposure to ionizing radiation due to naturally occurring radionuclides on man have been a cause of concern. It has been reported that natural radionuclides contribute about 23% of the average annual dose to man (NCRPM, 1987). The natural environment is made of indoor exposure to radon (Yu et al, 1993; 1996) and outdoor exposure to gamma radiation of both terrestrial and cosmic origin (Delaune et al, 1986; Eisenbud, 1987). Apart from these external sources, internal sources of natural radiation have been noted (Feldman, 1977; Ban-nai et al, 1994; Komamura et al, 1994). Activity concentrations of ^{137}Cs and ^{40}K in foodstuffs consume in Egypt (Badran et al, 2003) Foliar uptake of radionuclides in strawberry as function by leaf age (Fortunati et al, 2004). These research activities in other parts of the world have led to concrete regulations and legislatures by government and regulatory bodies in those parts of the world.

The data needed for the assessment of the radiation level of most parts of Nigeria are scanty. Agu (1965) carried out one of the pioneering radiation monitoring exercises in Nigeria in 1965. Since then, work had progressed slowly in this area. The work done so far includes, atmospheric radioactivity of Tin mining by-product in Jos (Babalola, 1984; Oresegun and Babalola, 1990), ^{222}Rn in groundwater of Nigeria (Farai and Sanni, 1992a; 1992b), natural radionuclide content of some foodstuffs in Nigeria (Olomo, 1990; Arogunjo, 2003), natural radionuclide concentrations in aquatic species (Farai and Oni, 2002), and the determination of natural radionuclide contents of soil and rocks in some parts of Nigeria (Olomo, et al 1994; Jibri and Farai, 1998; Arogunjo and Farai, 1999; Ajayi, 2000). Most of the works carried out in Nigeria are without particular focus on areas in this study

2.10 Effects of Ionizing Radiation on Human Tissue

The human body is made up of many organs, and each organ of the body is made up of specialized cells. Ionizing radiation can potentially affect the normal operation of these cells. In this section, we will discuss the potential for biological effects and risks due to ionizing radiation. Biological effects begin with the ionization of atoms. The mechanism by which radiation causes damage to human tissue, or any other material, is by ionization of atoms in the material. Ionizing radiation absorbed by human tissue has enough energy to remove electrons from the atoms that make up molecules of the tissue. When the electron that was shared by the two atoms to form a molecular bond is dislodged by ionizing radiation, the bond is broken and thus, the molecule falls apart. This is a basic model for understanding radiation damage. (NRPB, 2004) When ionizing radiation interacts with cells, it may or may not strike a critical part of the cell. We consider the chromosomes to be the most critical part of the cell since they contain the genetic information and instructions required for the cell to perform its function and to make copies of itself for reproduction purposes. Also, there are very effective repair mechanisms at work constantly which repair cellular damage - including chromosome damage. The following are possible effects of radiation on cells:

1 Cells are undamaged by the dose

Ionization may form chemically active substances which in some cases alter the structure of the cells. These alterations may be the same as those changes that occur naturally in the cell and may have no negative effect.

2 Cells are damaged, repair the damage and operate normally

Some ionizing events produce substances not normally found in the cell. These can lead to a breakdown of the cell structure and its components. Cells can repair

the damage if it is limited. Even damage to the chromosomes is usually repaired. Many thousands of chromosome aberrations occur constantly in our bodies. We have effective mechanisms to repair these changes.

3 Cells are damaged, repair the damage and operate abnormally

If a damaged cell needs to perform a function before it has had time to repair itself, it will either be unable to perform the function or perform the function incorrectly or incompletely. The result may be cells that cannot perform their normal functions or that now are damaging to other cells. These altered cells may be unable to reproduce themselves or may reproduce at an uncontrolled rate. Such cells can be the underlying causes of cancers.

4 Cells die as a result of the damage

If a cell is extensively damaged by radiation, or damaged in such a way that reproduction is affected, the cell may die. Radiation damage to cells may depend on how sensitive the cells are to radiation.

All cells are not equally sensitive to radiation damage. In general, cells which divide rapidly and/or are relatively non-specialized tend to show effects at lower doses of radiation than those which are less rapidly dividing and more specialized. Examples of the more sensitive cells are those which produce blood. This system (called the hemopoietic system) is the most sensitive biological indicator of radiation exposure. Potential biological effects depend on how much and how fast a radiation dose is received. Radiation doses can be grouped into two categories, *acute* and *chronic* dose.

2.10.1 Acute dose

An acute radiation dose is defined as a large dose (10 rad or greater, to the whole body) delivered during a short period of time (on the order of a few days at the most). If large enough, it may result in effects which are observable within a period of hours to weeks. Acute doses can cause a pattern of clearly identifiable symptoms (syndromes). These conditions are referred to in general as *Acute Radiation Syndrome*. Radiation sickness symptoms are apparent following acute doses ≥ 100 rad. Acute whole body doses of ≥ 450 rad may result in a statistical expectation that 50% of the population exposed will die within 60 days without medical attention.

Blood-forming organ (Bone marrow) syndrome (>100 rad) is characterized by damage to cells that divide at the most rapid pace (such as bone marrow, the spleen and lymphatic tissue). Symptoms include internal bleeding, fatigue, bacterial infections, and fever.

Gastrointestinal tract syndrome (>1000 rad) is characterized by damage to cells that divide less rapidly (such as the linings of the stomach and intestines). Symptoms include nausea, vomiting, diarrhea, dehydration, electrolytic imbalance, and loss of digestion ability, bleeding ulcers, and the symptoms of blood-forming organ syndrome.

Central nervous system syndrome (>5000 rad) is characterized by damage to cells that do not reproduce such as nerve cells. Symptoms include loss of coordination, confusion, coma, convulsions, shock, and the symptoms of the blood forming organ and gastrointestinal tract syndromes. Scientists now have evidence that death under these conditions is not caused by actual radiation damage to the nervous system, but rather from complications caused by internal bleeding, and fluid and pressure build-up on the brain.

Other effects from an acute dose include

125 to 200 rad to the ovaries can result in prolonged or permanent suppression of menstruation in about fifty percent (50%) of women.

200 to 300 rad to the skin can result in the reddening of the skin (erythema), similar to mild sunburn and may result in hair loss due to damage to hair follicles.

600 rad to the ovaries or testicles can result in permanent sterilization. 50 rad to the thyroid gland can result in benign (non cancerous) tumors. As a group, the effects caused by acute doses are called deterministic. Broadly speaking, this means that severity of the effect is determined by the amount of dose received. Deterministic effects usually have some threshold level - below which, the effect will probably not occur, but above which the effect is expected. When the dose is above the threshold, the severity of the effect increases as the dose increases.

2.10.2 Chronic dose

A chronic dose is a relatively small amount of radiation received over a long period of time. The body is better equipped to tolerate a chronic dose than an acute dose. The body has time to repair damage because a smaller percentage of the cells need repair at any given time. The body also has time to replace dead or non-functioning cells with new, healthy cells. This is the type of dose received as occupational exposure. The biological effects of high levels of radiation exposure are fairly well known, but the effects of low levels of radiation are more difficult to determine because the deterministic effects described above do not occur at these levels. Since deterministic effects do not generally occur with chronic dose, in order to assess the risk of this exposure, we must look to other types of effects. Studies of people who have received high doses have shown a link between radiation dose and some delayed, or *latent* effects. These effects include some forms of cancer and genetic effects (Knoll, 1989).

CHAPTER THREE

3.1 RADIATION DETECTION AND MEASUREMENT

The interaction of either charged or uncharged radiation involves the transfer of energy of the incident radiation either fully or partially to the electrons or nucleus of the constituent atoms of the interacting medium. Gamma rays interact with matter in three principal ways, which are: photoelectric absorption, Compton scattering and pair production. This will be discussed in this section, as this is the basis of the γ -spectrometric method employed in this work.

3.1.1 Photoelectric Absorption

Photoelectric effect is an interaction between a photon and a tightly bound electron whose binding energy is equal to or less than the energy of the photon. In this process, a photon of energy E_γ is absorbed by a bound electron. This leads to ejection of the electron from its orbit with energy T given by:

$$T = E_\gamma - E_b \quad 3.1$$

where, E_b is the binding energy of the electron. The primary ionic particle resulting from this interaction is the photoelectron. Equation 3.1 shows that photoelectron production occurs only when E_γ is equal to or greater than the binding energy of the electron in the absorbing materials. A vacancy is created mostly from the innermost shell (e.g. K-shell) due to the production of photoelectrons. This is promptly filled by electron from the higher energy shells with the emission of characteristic x-ray. The probability that photoelectric absorption will occur is expressed by the equation:

$$\tau = \frac{k\rho Z^3}{E^3} \quad 3.2$$

where k = a constant

Z = the atomic number of the absorbing material

ρ = the density of the absorbing material,

E = photon energy

Equation 3.2 shows that low energy photons and high atomic numbered absorbers favor the photoelectric effect. It is this very strong dependence of photoelectric absorption on the atomic number Z that makes Pb a good material for shielding against γ -rays. Sodium iodine crystal has high photoelectric absorption efficiency because of its high atomic number. This explains its popular choice in scintillation detection as employed in this work.

3.1.2 Compton Scattering

Compton scattering involves an elastic collision between a photon and a free or loosely bound electron. After the collision, the photon is scattered at angle θ to its initial direction and with less energy or a longer wavelength than the incident photon. The photon transfers the rest of its energy to the electron (assumed to be initially at rest), which thereafter moves away at some other angle. The amount of energy transferred in the collision can be calculated by applying the law of conservation of energy and momentum.

The energy E'_γ of scattered photon has been shown to be given by:

$$E'_\gamma = \frac{E_\gamma}{1 + \frac{E_\gamma}{m_e c^2} (1 - \cos\theta)} \quad 3.3$$

where E_γ is the initial photon energy and m_e is the electron rest mass. The scattered electron is the vehicle by which energy from the scattered photon is transferred to the absorbing medium. The kinetic energy T of the recoil electron is given by:

$$T = \frac{E_\gamma}{1 + \left(\frac{E_\gamma}{m_e c^2} (1 - \cos \theta) \right)^2} \quad 3.4$$

It can be seen from equation 3.4 that the minimum value of T is zero when $\theta = 0^\circ$ and the maximum value referred to as Compton edge, E_c is always less than the photon energy and it corresponds to a head-on collision in which the photon is scattered back wards that is $\theta = 180$ in this case:

$$E_c = E_\gamma \left[\frac{2E_\gamma}{m_e c^2 + 2E_\gamma} \right] \quad 3.5$$

Equation 3.4 shows that a continuum of energies can be transferred to the electron ranging from zero up to the maximum given by equation 3.5. This explains the continuous distribution of pulse heights termed Compton plateau in gamma spectroscopy.

3.1.3 Pair production

When a photon of energy greater than 1.02 MeV, comes near the nucleus of an atom, it is subjected to the strong field of the nucleus. It may disappear and become a positron and an electron. The energy equation of the process is given by

$$h\nu = E_{e^+} + E_{e^-} + 2m_e c^2 \quad 3.6$$

where E_{e^+} and E_{e^-} are the kinetic energies of the emitted positron and electron respectively. Equation 3.6 implies that pair production can take place only if $h\nu \geq 2m_e c^2$ (1.02 MeV). The positron produced is a very unstable particle. Once its kinetic energy becomes zero it interact with an electron almost immediately, thereby annihilating each other to form two 0.511 MeV photons which travel in opposite directions. These may escape from the medium or interact with it in Compton or photoelectric processes. This usually leads to a photo peak at 0.511 MeV, which can be confused with the gamma peaks being measured especially if the source has gamma energy close to 0.511 MeV.

Unlike the other two interactions, pair production has a cross-section σ_{pp} , which increases, although slowly, with photon energy E_γ and the interaction tend to be dormant at high energies. The cross-section can be written as:

$$\sigma_{pp} = cZ^2 \rho \ln E_\gamma \quad 3.7$$

where, c = a constant. The net effect of the above three processes is an exponential attenuation in the intensity of a beam of gamma rays passing through a thickness x of an absorbing materials. This is described by the equation:

$$I = I_0 e^{-\sigma x} \quad 3.8$$

Where I_0 = the initial intensity at $x = 0$, σ = the absorption co-efficient due to all the effects.

3.2 SCINTILLATION DETECTION

Scintillation mechanism in inorganic scintillators depends on the energy states of the crystal lattice. The valence band contains electrons, which are bound to the lattice sites. The conduction band contains electron with sufficient energy to move freely. Between the two energy bands, there is the forbidden gap where electrons cannot be found in a pure crystal. When the incident photon interacts with the scintillators through one or more of the processes discussed in 3.1, an electron acquires enough energy to move from the valence band to the conduction band. The subsequent de-excitation of the electron to original state, results in the emission of the photon energy that may be too high to lie within the visible photon emission during de-excitation, in order to enhance the probability of visible photon emission during de-excitation, impurity (activator) such as thallium is added to the sodium iodide crystal. This creates special sites to modify the energy band of the crystal. The excitation takes the electrons to any of the energy state created within the forbidden gap, resulting in photon emission in the visible range.

The modern-day photomultiplier (PM) tube converts the light into an electrical pulse, which may be amplified, sorted by size and counted. Scintillation detectors are widely used for the detection and spectroscopy of gamma rays and low energy beta rays.

The detector most frequently used for gamma-ray counting is a sodium iodide crystal activated with thallium NaI (TI) optically coupled to the photomultiplier tube. This is because of its density (higher probability for photoelectric interaction) as shown in equation 2.5 and high effective atomic number (due to iodine). Sodium iodide crystal is highly hygroscopic which results in the crystal deterioration when exposed to moisture. Therefore, the crystal is hermetically sealed in light proof covering, usually by a light metal, with an optical window through which it is then coupled to a photomultiplier tube. A Canberra 76 mm x 76mm NaI (TI) detector was used for the radioactivity measurements of the vegetable samples in this work. The systematic detection processes by the NaI (TI) detector assembly is described below;

3.2.1 Scintillation detection by NaI (TI)

A schematic representation of the sequence of events in the detection of a gamma ray photon by a scintillation detection system is shown in fig. 3.1. When an energetic charge particle is incident on the crystal, the primary ionizing particles resulting from the gamma-ray interactions dissipate their kinetic energy by exciting and ionizing the atoms in the crystal. The high Z of iodine in NaI results in high efficiency for gamma-ray detection. A small amount of TI is added in order to activate the crystal, so that the designation is usually NaI (TI) for the crystal.

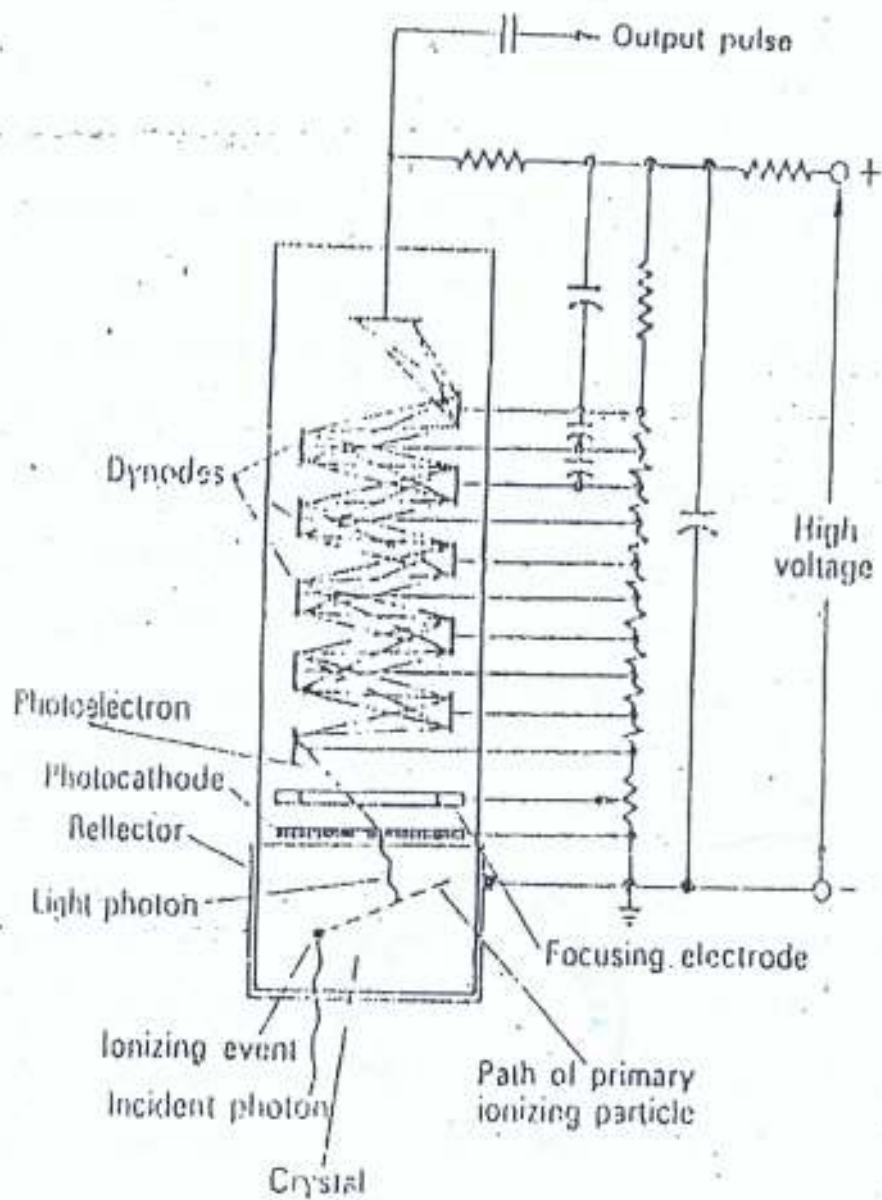


Fig 3.1 Schematic Representation of the Sequence of events in the detection of a gamma ray Photon by a scintillation detection system (Knoll,1989)

3.2.2 Photomultiplier Tube

A Photomultiplier tube [PMT] is a sensitive device for measuring photon counts, and is used in a wide variety of applications. Because of its sensitivity, it is susceptible to the influences of a number of external parameters, such as electric fields, magnetic fields, and temperature. Because it operates using the photoelectric effect, the PMT also shows a small dark current produced by the thermal emission of electrons from its cathode. Among the photosensitive devices in use today, the photomultiplier tube (or PMT) is a versatile device that provides extremely high sensitivity and ultra-fast response. A typical photomultiplier tube consists of a photoemissive cathode (photocathode) followed by focusing electrodes, an electron multiplier and an electron collector (anode) in a vacuum tube. When light enters the photocathode, the photocathode emits photoelectrons into the vacuum. The process of secondary emission multiplies these photoelectrons. The anode collects the multiplied electrons.

Because of secondary-emission multiplication, photomultiplier tubes provide extremely high sensitivity and exceptionally low noise among the photosensitive devices currently used to detect radiant energy in the ultraviolet, visible, and near infrared regions. The photomultiplier tube also features fast time response, low noise and a choice of large photosensitive areas. The photograph of photomultiplier tube is shown in Figure 3.2.



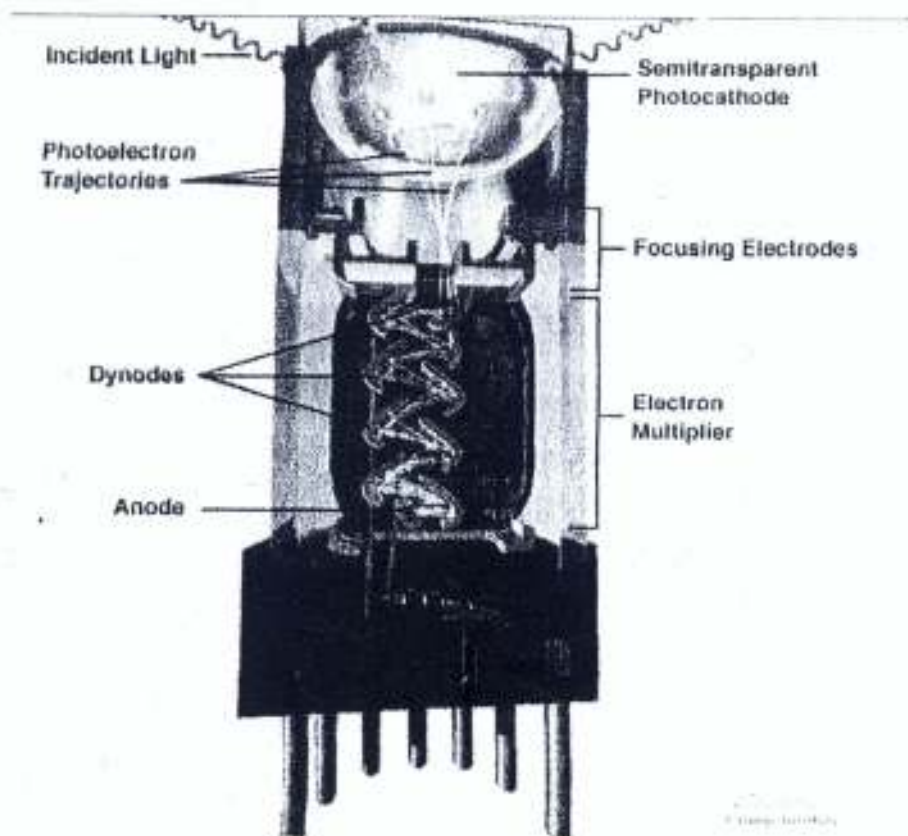


Fig.3.2 Photomultiplier Tube (<http://www.cord.org/step-online>)

3.2.3 Pulse Shaping and Height Analysis

The number of electrons that reach the anode (or collection) decays according to the equation:

$$N = Q e^{-\frac{t}{T_d}} \quad 3.9$$

Where T_d is the modified decay time of the scintillant which is about 0.25 μsec for NaI (TI). Because of the short lifetime of the pulses, they may be subjected to a pile up and as such, it is important to collect information about a pulse as quickly as possible. A pulse shaping RC circuit function is to preserve maximum information while reducing the pulse duration usually used to achieve this. The RC circuit as shown in Figure 3.3 is usually placed after the amplifier. The number of electrons

$N(t)$ in the shaped output is given by Birks (1964) as:

$$N(t) = Q \left[\frac{RC}{RC - T_d} \right] \left[e^{-\frac{t}{RC}} - e^{-\frac{t}{T_d}} \right] \quad 3.10$$

The voltage is, thus, given by:

$$V(t) = \frac{Qe}{C_s} \left[\frac{RC}{RC - T_d} \right] \left[e^{-\frac{t}{RC}} - e^{-\frac{t}{T_d}} \right] \quad 3.11$$

Equation 3.10 shows that the amplitude of the pulse depends on C , T_d and RC (time constant) of the circuit. The RC must be greater than T_d to ensure that $V(t)$ peak is proportional to the energy dissipated by the primary radiation in the scintillator. In essence, the pulse height is maximized and subsequent noise will have minimum degrading effect.

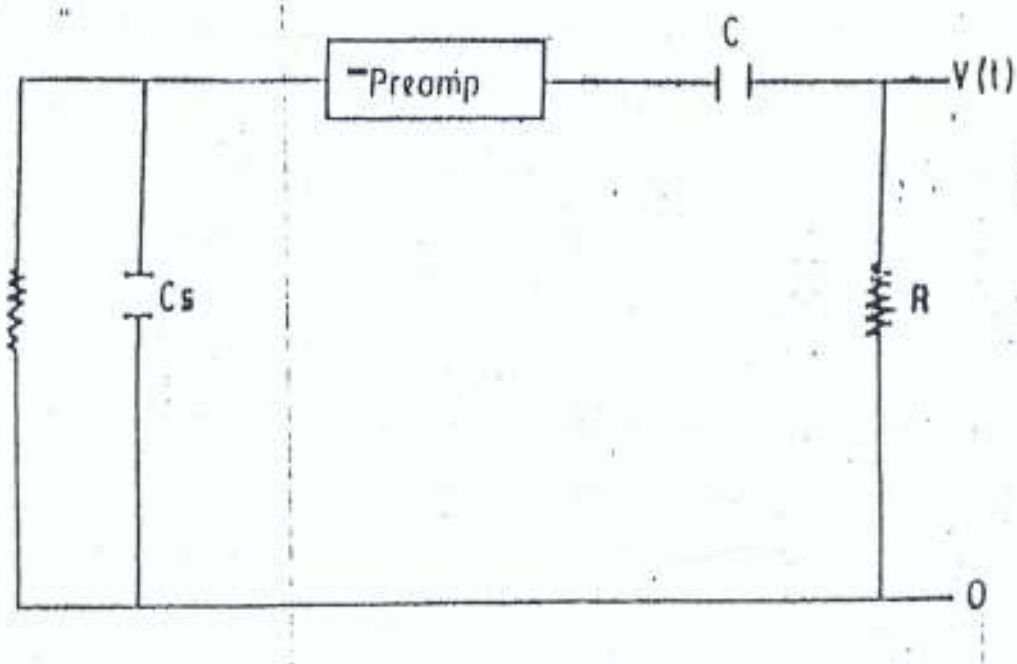


Fig. 3.3 A Schematic Representation of a Pulse Shaping Circuit

2.8 RESOLUTION

As a result of statistical fluctuations in the various factors leading to its production, a photopeak is usually a Gaussian spread around the peak energy. It is therefore possible for the spread of one photopeak to overlap with that of another if they are too close. The ability of a detector assembly to distinguish between two energies that are close is termed resolution, R . The width of this distribution is a measure of the resolution of the spectrometric system. In gamma spectrometry, resolution R is defined quantitatively as the full width at half maximum (FWHM) divided by the photopeak centroid E_o , that is:

$$R = \frac{FWHM}{E_o} \times 100\% \quad 3.12$$

The typical resolution of a 76mm x 76mm NaI (TI) detector is 5–10% depending on the energy of gamma radiation (Thompson et al, 1999). Although this resolution is low when compared with those obtained from Ge(Li) or HPGe detector, it has proved adequate as shown in Figure 3.4, in distinguishing the photopeaks due to the primordial radionuclide in the samples. Figure 3.4 has been obtained by counting ^{40}K , ^{238}U and ^{232}Th standard sources separately under laboratory condition, in order to show the photopeaks that stand out and hence, can be resolved by the detector. The spectra show ^{238}U and ^{232}Th with many photopeaks corresponding to different energies (609keV, 1238keV and 1764keV for ^{238}U ; 583keV and 2614keV ^{232}Th) due to different gamma emitting progeny of these elements. From Figure 3.4 the gamma ray peaks used for ^{40}K , ^{238}U and ^{232}Th were 1460keV, 1764keV due to ^{214}Bi and 2614keV due to ^{208}Tl , respectively since the photopeaks stand out in all the spectrum of the samples. These photopeaks are then used as the indicators of the specific activity of the radionuclides.

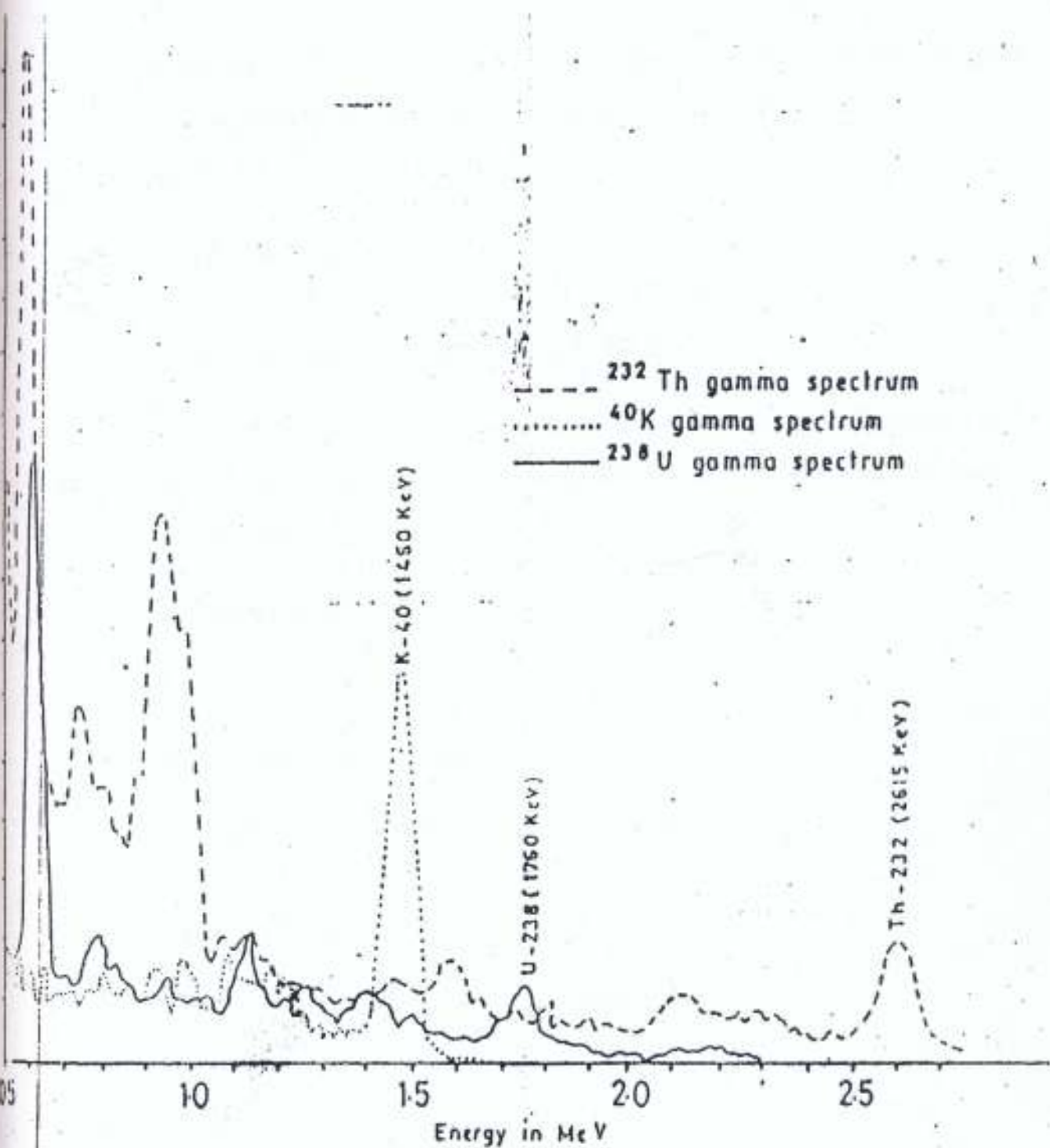


Fig. 3.4 The gamma spectra of the primordial radionuclides

3.4 NET AREA CALCULATION

When a peak lies on a background that cannot be subtracted by a background spectrum, such as shown in Figure 3.5 for an MCA spectrum from a detector: the area above the background represents the total counts between the vertical lines minus the trapezoidal area below the straight line. If the total count is P and the points of the straight line are B_1 and B_2 , then the net area is given by:

$$A = P - \frac{n}{2} (B_1 + B_2) \quad 3.13$$

where n = the number of channels between B_1 and B_2 .

The errors in B_1 and B_2 affect the straight line across the entire region. Equation 3.13 is implemented in Canberra MCAs in analysis of peak areas in software packages, which is derived as follows:

The standard deviation in a function A is given by:

$$A = f(N_1 N_2 \dots N_n)$$

where N_n is the counts in channel N .

The estimate of the standard deviation in A is given by:

$$\begin{aligned} \sigma(A) &= \left[\left(\frac{\partial f}{\partial N_1} \right)^2 \sigma^2(N_1) + \dots + \left(\frac{\partial f}{\partial N_n} \right)^2 \sigma^2(N_n) \right]^{1/2} \\ &= \left[(P_1 + \dots + P_n) + \left(\frac{n}{2} \right)^2 (\sqrt{B_1})^2 + \left(\frac{n}{2} \right)^2 (\sqrt{B_2})^2 \right]^{1/2} \\ &= \left[P + \left(\frac{n}{2} \right)^2 (B_1 + B_2) \right]^{1/2} \end{aligned} \quad 3.14$$

where $P_1 \dots P_n$ are the channels in the peak (inside B_1 and B_2).

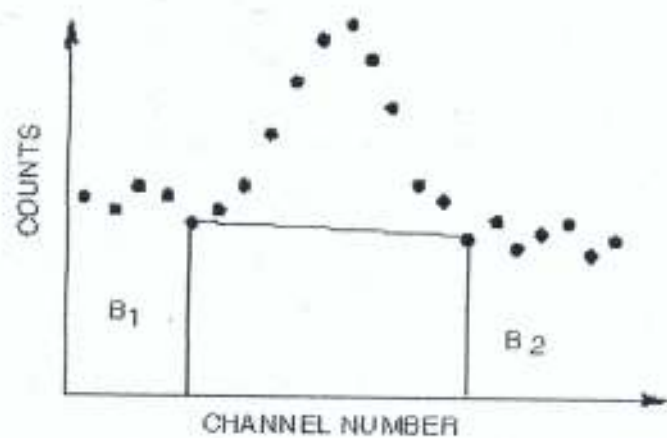


Fig. 3.5 Net Area Determination

3.4.1 End-Point Averaging

If the background is large compared to the peak area, a better determination of background can be made by averaging over several channels. If B_1 is the sum of counts over n_1 channels and B_2 over n_2 channels, the area is then:

$$A = P - \frac{n}{2} \left(\frac{B_1}{n_1} + \frac{B_2}{n_2} \right)$$

and the standard deviation is:

$$\sigma(A) = \left[P + \left(\frac{n}{2} \right)^2 \left(\frac{B_1}{n_1^2} + \frac{B_2}{n_2^2} \right) \right]^{1/2}$$

3.15

Most Canberra MCAs and analysis software packages perform end-point averaging with a user-selectable number of end-points.

3.5 GAMMA-RAY SPECTROMETRY

Gamma –spectrometry is a technique of analyzing the energy of the gamma-radiation emitted by a nuclide, to permit conclusion to be drawn on the type of nuclide or nuclide mixture. A gamma spectrometer consists of a detector preamplifier and detector bias supply, pulse height analyzer system, data readout capability and shielded sample enclosure. The pulse-height analyzer system consists of a linear amplifier, an analog-to digital converter (ADC) memory storage and a logic control mechanism. The logic control capabilities allow data storage in various modes and display or recall of data. All spectrometry measurements made to date use either NaI (TI) or germanium (Ge) detector (Thompson et al., 1999).

The three common processes of energy transfer by gamma-rays have been discussed in section 2.5. The fast electrons, which result from these processes, provide very useful information on energy and intensity of the incident gamma-rays. The system for the conversion of these fast electrons into flash of light, detected by optically matched electronic system to yield useful information concerning the primary γ -photon constitute scintillation γ -ray spectroscopic system. The ability of the system to differentiate between radiation energies and hence, identify sources in the environment is the basis of its application in this work.

CHAPTER FOUR

MATERIALS AND METHOD

4.1 Calibration

Radioactivity counting in this work was carried out using a lead shielded 76mm x 76mm NaI (TI) detector crystal (Model No 802 Series) by Canberra Inc., which is coupled to a Canberra series plus 10 Multichannel Analyzer (MCA) (Model No 1104) through a preamplifier base. Figure 4.1 shows a schematic diagram of the measuring assembly. The calibration of the detector system was done in two ways. The first was to convert the channel numbers to gamma ray energy in MeV and the second was to determine efficiencies at different γ -energies. The two steps are discussed below;

4.1.1 Energy Calibration

Using a set of standard gamma emitters from IAEA with energies in the range of 0.511-2.62 MeV for the calibration of the detector system to determine the equation relating energy to the channel number. After a preset counting time of 36000s, the channel numbers of the photopeaks corresponding to different gamma energies were identified. Using energy calibration (ECAL) function of the MCA, the linear relationship fitting the graph was obtained as:

$$Y = 0.8418X + 43.418 \quad 4.1$$

The energy- channel linear relationship is shown in Figure 4.2. With equation 4.1, using Table 4.1, the detection system could therefore be used to identify an unknown source from the channel number corresponding to the gamma energy it emits.

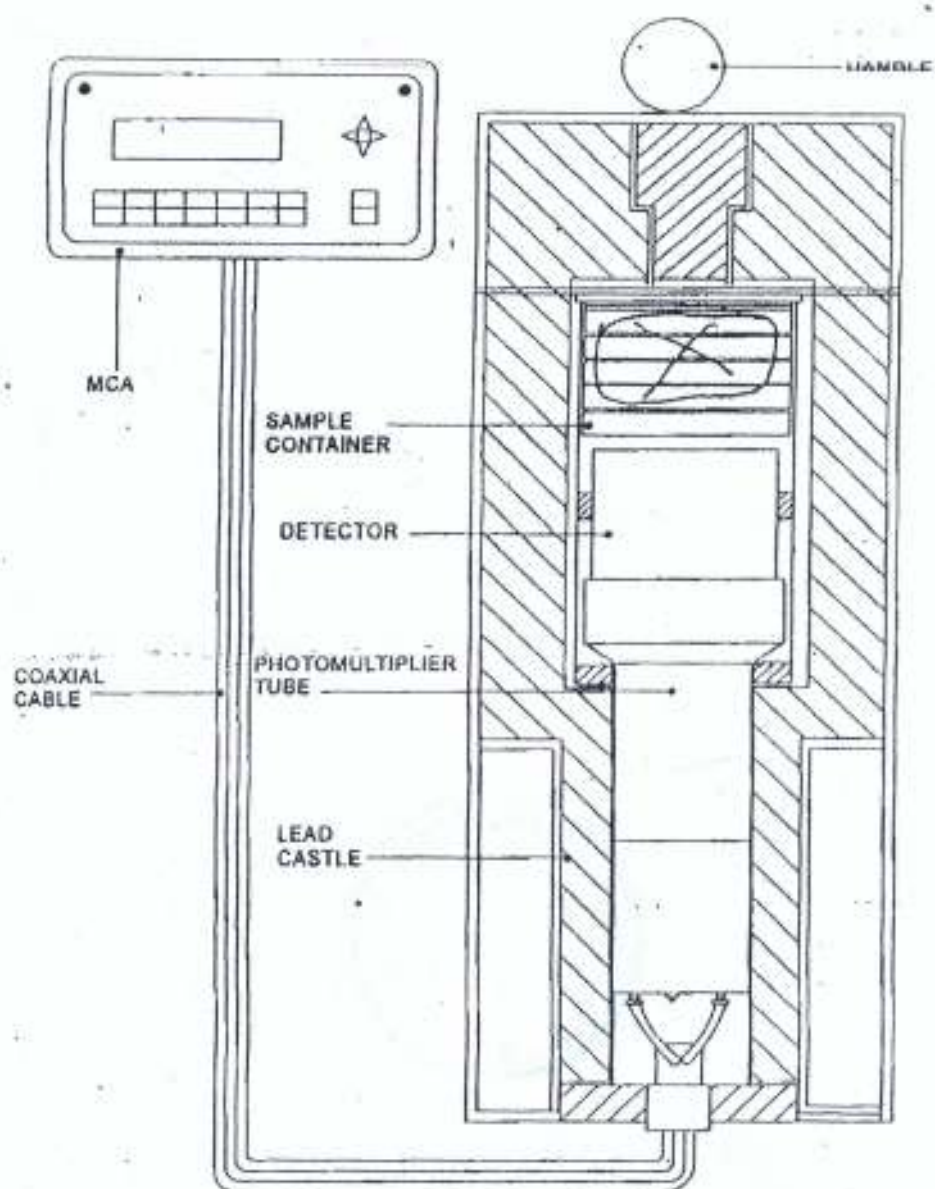


Fig 4.1 Schematic Diagram of the Measuring Assembly.

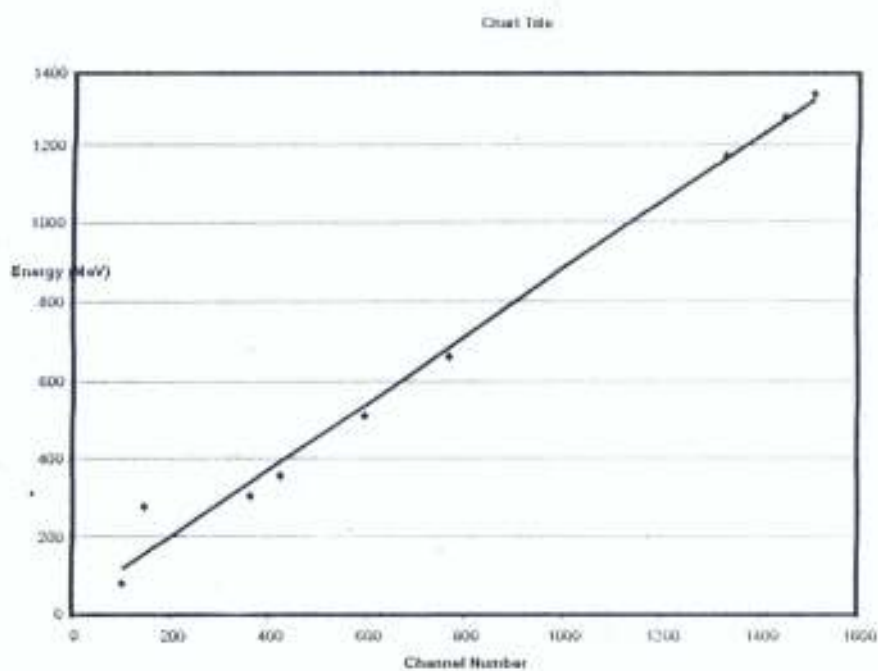


Fig 4.2 Graph showing energy-channel dependence



Table 4.1 Energy Channel linear relationship

| Energy (Kev) | Channel |
|--------------|---------|
| 81.00 | 102.47 |
| 276.39 | 145 |
| 302.85 | 362 |
| 356.01 | 424 |
| 511 | 595 |
| 1274.54 | 1448 |
| 661.66 | 767.21 |
| 1173.24 | 1330.50 |
| 1332.50 | 1508.53 |

4.1.2 Efficiency Calibration

Calibration of the efficiency of the system against gamma ray energies was achieved using a certified reference source sample traceable to source number IAEA International Reference 375 January 2000. The reference source was counted for 10 hours (36000s) after which the detector efficiencies at the different γ energies were calculated using the equation below (Farai and Sanni, 1992)

$$\varepsilon_{\gamma} = \frac{C_{\text{net}}}{A_s Y_{\gamma} m_s} \quad 4.2$$

where,

ε_{γ} is the efficiency of the detector

C_{net} is the net counts per second above the background

A_s is the activity of standard source at a particular γ - energy (Bqkg^{-1})

Y_{γ} is the intensity of gamma ray at the particular energy being counted

m_s is the mass of the sample

The values of the efficiencies are presented in Table 4.1 while the efficiency curve is shown in Figure 4.3. It can be observed from the curve that the efficiency of the detector decreases with γ -ray energies. This may be attributed to the escape of secondary photon resulting from complex types of interaction at high γ energies with the detector crystal

Table 4.2 Detector efficiencies at different γ -energies

| Radionuclides | Energy (MeV) | Gamma yield | Efficiency ($\times 10^{-2}$ cps/Bq) | Factor <i>f</i> |
|-------------------|-----------------|----------------|--|--------------------|
| ^{40}K | 1.460 | 0.107 | 1.87 | 1923.7 |
| ^{238}U | 1.764 | 0.159 | 1.67 | 1695.5 |
| ^{232}Th | 2.614 | 0.358 | 1.35 | 632.8 |

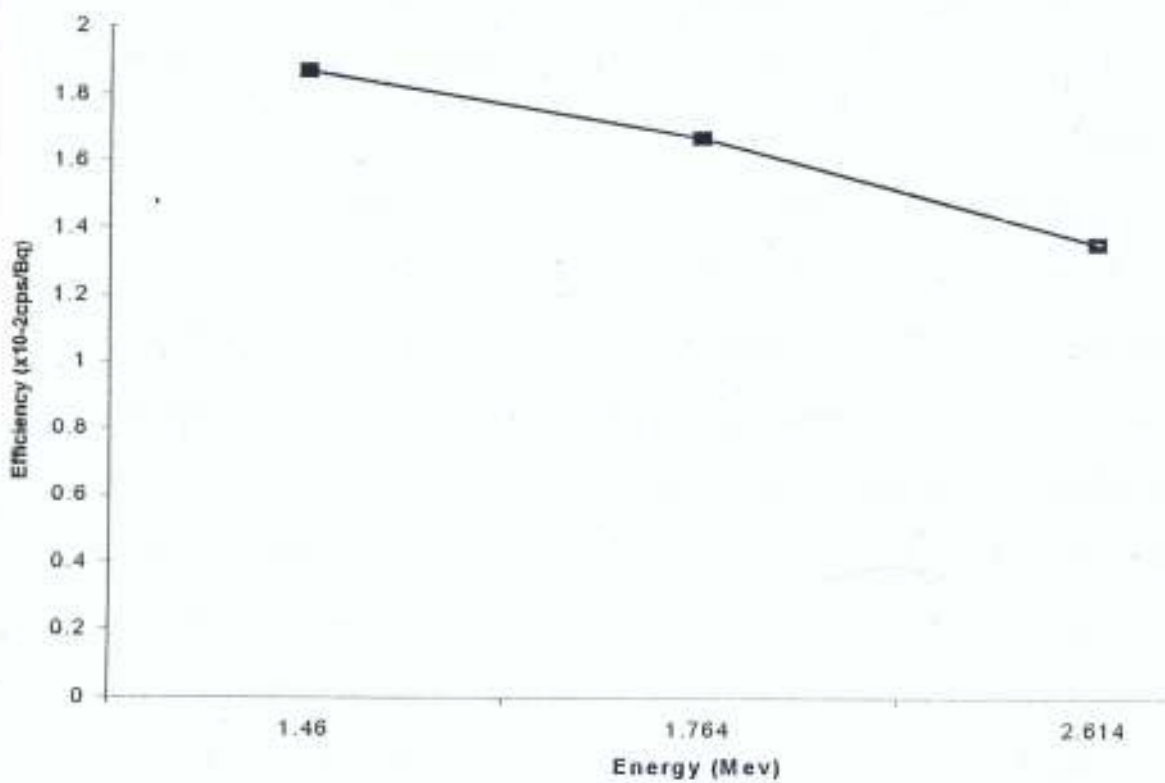


Fig. 4.3: The Efficiency of the system as a function of gamma energy

4.2 SAMPLE COLLECTION AND PREPARATION

The criteria for selection of the vegetables were to represent different vegetable types that are commonly consumed by the people in each location. Table 3.2-3.4 shows the vegetables analyzed in three locations in this work together with their botanical names. The study investigated the concentrations of radionuclides in vegetables collected from three towns in Ondo State, namely Jegele (7°N , 5°E), Idanre (9°N , 7°E) and Agbabu (6°N , 4°E). Agbabu is a bitumen-rich producing area, Idanre, being a rocky settlement, is expected to be high in radioactivity while Jegele village is a local settlement used as control site. Forty - nine (49) samples of seven (7) species vegetables, which were cultivated in each of the three locations, were purchased from local farmers. The whole plant was not used in the measurements but only the edible portions were used (IAEA, 1989). The vegetables were hand cleaned to remove soil particles and then washed with tap water contained in a basin. The samples were weighed fresh, dried at 80°C in the oven until it attained constant weight. The dried samples were packed in 50g lots by weight and hermetically sealed in plastic container, which have been verified to be non radioactive. They were thereafter left for 28 days in order for the gaseous daughters of U and Th series to reach secular equilibrium before counting.

Table 4.3 Vegetables investigated in Jegele with their botanical names

| Sample Number | Local Names | Botanical Names |
|----------------|-------------|------------------------|
| C ₁ | Tete | Amaranthus spp |
| C ₂ | Ugwu | Telfairia Occidentalis |
| C ₃ | Gbure | Talium Triangulare |
| C ₄ | Ewuro | Venonia amygdalina |
| C ₅ | Igbo | Solanium macncarpon |
| C ₆ | Rorowo | African spinach |
| C ₇ | Ewedu | Corchorous Olitorius |

Table 4.4 Vegetables investigated in Idanre with their botanical names

| Sample Number | Local Names | Botanical Names |
|----------------|-------------|------------------------|
| C ₁ | Tete | Amaranthus spp |
| C ₂ | Ugwu | Telfairia Occidentalis |
| C ₃ | Gbure | Talium Triangulare |
| C ₄ | Ewuro | Venonia amygdalina |
| C ₆ | Rorowo | African spinach |

Table 4.5 Vegetables investigated in Agbabu with their scientific names

| Sample Number | Local Names | Botanical Names |
|----------------|-------------|------------------------|
| C ₁ | Tete | Amaranthus spp |
| C ₂ | Ugwu | Telfairia Occidentalis |
| C ₃ | Gbure | Talium Triangulare |
| C ₄ | Ewuro | Venonia amygdalina |
| C ₅ | Igbo | Solanium macncarpon |
| C ₇ | Ewedu | Corchorous Oitorius |

4.3 RADIOACTIVITY COUNTING

Radioactivity counting of the samples was done on the detector system, which had been calibrated as described in section 4.1.1 and 4.1.2. The counting time for each sample was 36,000s (10hrs) after which the area (A) under each photopeak of the radionuclides was computed using the algorithm of the MCA (equations 3.13-3.15). The area under the photopeaks of each of the three primordial radionuclides was related to radioactivity concentration A_s of the samples (in Bqkg⁻¹) using equation 4.1 which for a source of unknown activity A_s can be written as

$$A_s = \frac{C_{net}}{\epsilon_\gamma Y_\gamma m_s} \quad 4.3$$

where,

ϵ_γ is the detector efficiency at the γ - energy

C is the count per second of the sample

Y_γ is the intensity of gamma ray at the particular energy being counted

m_s is the mass of the sample

CHAPTER FIVE

RESULTS AND DISCUSSION

5.1 ACTIVITY CONCENTRATIONS

The three primordial radionuclides, ^{40}K , ^{238}U and ^{232}Th were detected and measured in the seven (7) vegetable species collected from the three locations. The mean specific activity of the radionuclides for each location detected in the samples is presented in Tables 5.1-5.3. All the radionuclides detected and quantified came from the naturally occurring ^{238}U and ^{232}Th series decay with exception of ^{40}K . Which are mainly of ^{208}Tl and ^{214}Bi . The errors quoted along with each mean value is the standard deviation ($\pm \sigma$), which tells the extent of spatial spread on the concentration of the radionuclides in the vegetable samples within each location. The concentration of ^{40}K was scaled by factor of 1/15 so as to accommodate the values along side with those of ^{238}U and ^{232}Th on the same bar chart. This becomes necessary in order to facilitate good basis for comparisons. The obtained figures were shown figures in 5.1-5.3. The interpretations of the measured results are as follows;

5.1.1 Location 1: Jegele (7°N, 5°E)

Seven vegetable samples collected in location 1 i.e Jegele were analyzed. The mean radioactivity concentrations for ^{40}K , ^{238}U and ^{232}Th in each of the seven vegetables are presented in Table 5.1. Figure 5.1 is a bar chart representing the measured values. The highest concentrations of ^{40}K at this location was found in Gbure (*TatumTriagulare*) with value $2376.91 \pm 120.23 \text{ Bqkg}^{-1}$. Igbo (*Solanum macncarpon*) was found to have the highest level of ^{238}U (51.94 ± 39.40) Bqkg^{-1} , while Ewuro (*Vernonia Amygdahna*) was observed to contain highest ^{232}Th (14.48 ± 2.99) Bqkg^{-1} . The large values of standard deviation of ^{40}K in the location are as a result of large disparities in the values of this radionuclide within this location. The lowest activity concentrations of ^{40}K ($721.60 \pm$

36.44) Bqkg⁻¹ was obtained in Ugwu (*Telfairia Occidentalis*), Ewedu (*Corchorous Olitorious*) has the lowest concentration of ²³⁸U (2.38 ± 0.14) Bqkg⁻¹, while the lowest concentration of ²³²Th (8.54 ± 1.71) Bqkg⁻¹ was obtained in Ugwu (*Telfairia Occidentalis*)

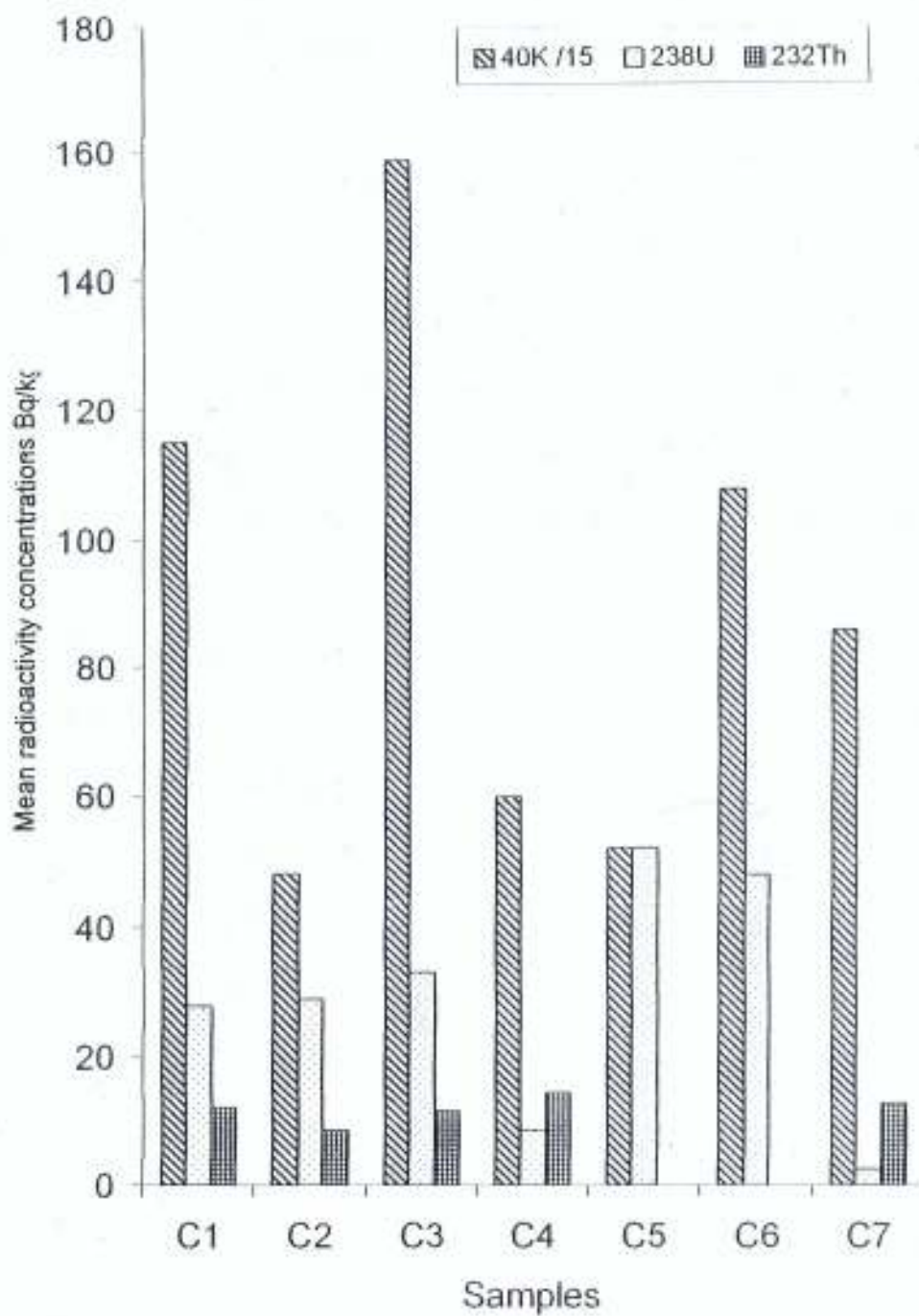


Fig. 5. 1. Mean radioactivity concentrations of ^{40}K , ^{238}U and ^{232}Th in location I (Jegele)

Table 5.1 Mean radioactivity concentrations of the radionuclides in location 1

| Sample | ^{40}K (Bqkg $^{-1}$) | ^{238}U (Bqkg $^{-1}$) | ^{232}Th (Bqkg $^{-1}$) |
|----------------|---------------------------------|----------------------------------|-----------------------------------|
| C ₁ | 1725.28 ± 85.44 | 27.96 ± 5.26 | 12.34 ± 1.83 |
| C ₂ | 721.60 ± 36.44 | 28.94 ± 5.26 | 8.54 ± 1.71 |
| C ₃ | 2376.91 ± 120.23 | 32.93 ± 4.60 | 11.71 ± 2.06 |
| C ₄ | 893.75 ± 44.19 | 8.56 ± 1.20 | 14.48 ± 2.99 |
| C ₅ | 779.54 ± 50.61 | 51.94 ± 39.40 | ND |
| C ₆ | 1613 ± 88.8 | 47.66 ± 17.16 | ND |
| C ₇ | 1287.00 ± 32.17 | 2.38 ± 0.14 | 12.83 ± 1.66 |

C₁= *Amaranthus spp*

C₂= *Telfairia Occidentalis*

C₃= *Talium Triangulare*

C₄= *Venonia amygdahna*

C₅= *Solanum macncarpon*

C₆= *African Spinach*

C₇ = *Corchorous Olitorius*

ND= Not Detectable

5.1.2 Location 2: Idanre (9°N, 7°N)

Five (5) samples of the species available during the dry season were collected and analyzed. The mean radioactivity concentrations of each vegetable are presented in Table 5.2 and Figure 5.2 is the bar chart representing the measured value. The highest concentrations of ^{40}K this location was found in Gbure (*Talium Triangulare*) with value $2459.73 \pm 62.72 \text{ Bqkg}^{-1}$. Gbure (*Talium Triangulare*) was found to have the highest level of ^{238}U (97.57 ± 5.28) Bqkg^{-1} , while Rorowo (*African Spinach*) was observed to contain highest ^{232}Th (18.44 ± 1.78) Bqkg^{-1} . The lowest concentration of ^{40}K (1075.07 ± 52.52) Bqkg^{-1} was found in Tete (*Amaranthus spp*), Ewuro (*Vernonia Amygdalhna*) has the lowest concentration of ^{238}U (25.12 ± 2.13) Bqkg^{-1} , while the lowest concentration of ^{232}Th (8.38 ± 1.1) Bqkg^{-1} was also obtained in Ewuro (*Vernonia Amygdalhna*). Here the lowest concentration is higher than other locations due to geological factor because the land is rocky which confirm the statement that igneous rocks are source of the primordial radionuclides. (www.umich.edu/info)

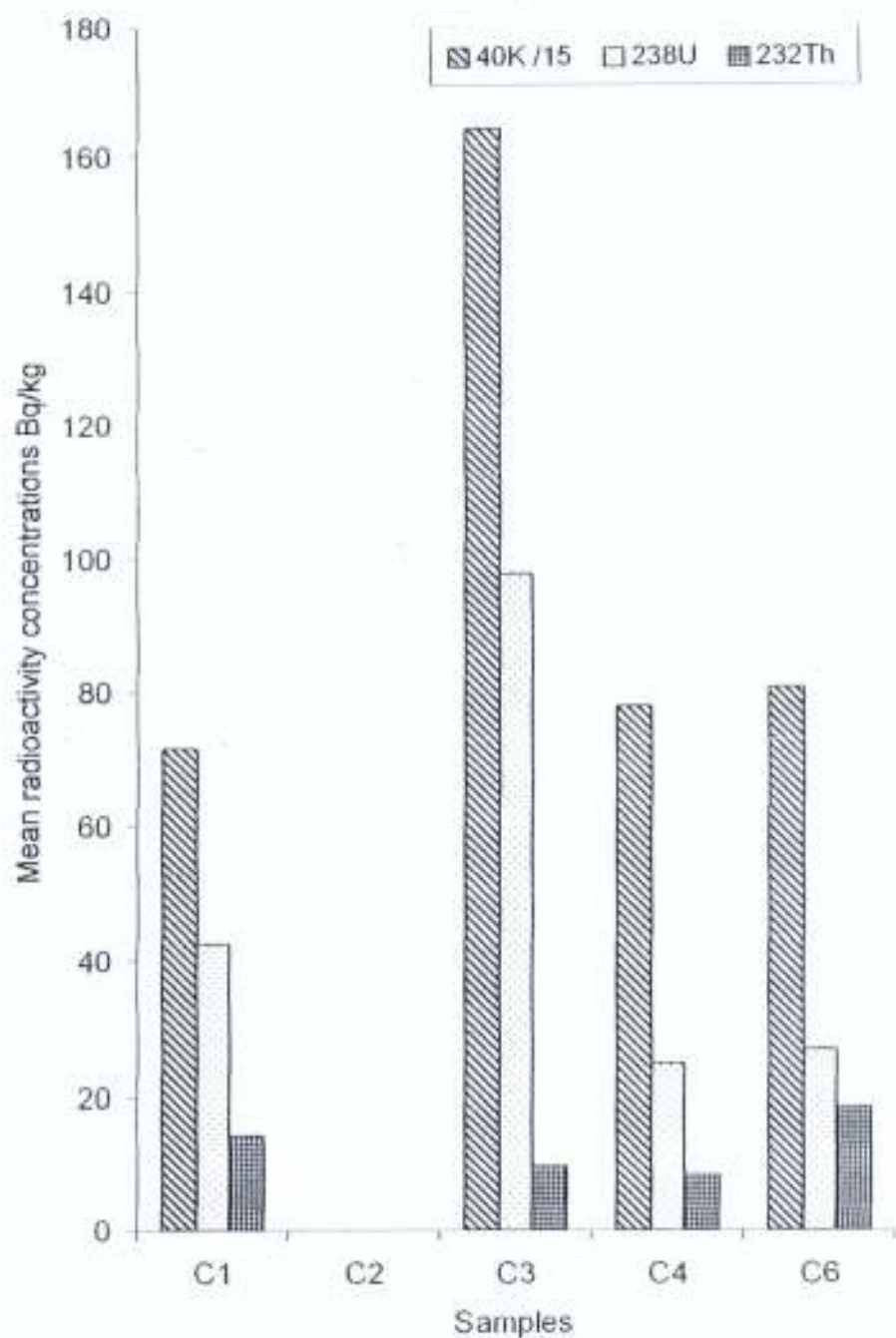


Fig. 5.2 Mean radioactivity concentrations of ^{40}K , ^{238}U and ^{232}Th in location 2 (Idamre)

Table 5.2 Mean radioactivity concentrations of the radionuclides in location 2

| Sample | ^{40}K (Bqkg $^{-1}$) | ^{238}U (Bqkg $^{-1}$) | ^{232}Th (Bqkg $^{-1}$) |
|----------------|---------------------------------|----------------------------------|-----------------------------------|
| C ₁ | 1075.07 ± 52.52 | 42.46 ± 3.80 | 14.34 ± 2.95 |
| C ₂ | ND | ND | ND |
| C ₃ | 2459.73 ± 62.52 | 97.57 ± 5.28 | 9.85 ± 0.94 |
| C ₄ | 1169.16 ± 30.31 | 25.01 ± 2.13 | 8.38 ± 1.11 |
| C ₆ | 1209.28 ± 90.52 | 26.75 ± 3.06 | 18.44 ± 1.78 |

C₁= *Amaranthus spp*

C₂= *Telfairia Occidentalis*

C₃= *Tatium Triangulare*

C₄= *Veronia amygdalina*

C₆= *African Spinach*

ND = Not Detectable

5.1.3 Location 3: Agbabu (6°N, 4°N)

Six different available vegetables in the season collected were analyzed. The mean radioactivity concentrations of each vegetable were presented in Table 5.3. Figure 5.3 is a bar chart that shows the representation of the measured values. The ^{40}K this location was found in Gbure (*Talium Triangulare*) with value $2208.69 \pm 60.60 \text{ Bqkg}^{-1}$. Gbure (*Talium Triangulare*) was found to have the highest level of ^{238}U (56.65 ± 2.83) Bqkg^{-1} , while Ugwu (*Telfairia Occidentalis*) was observed to contain highest ^{232}Th (15.99 ± 3.32) Bqkg^{-1} . The lowest concentration of ^{40}K (986.32 ± 50.73) Bqkg^{-1} was found in Ugwu (*Telfairia Occidentalis*), Igbo (*Solanium Macncarpon*) has the lowest concentration of ^{238}U (2.36 ± 0.54) Bqkg^{-1} , while the lowest concentration of ^{232}Th (6.23 ± 0.76) Bqkg^{-1} was obtained in Ewedu (*Corchorous Oltortious*).

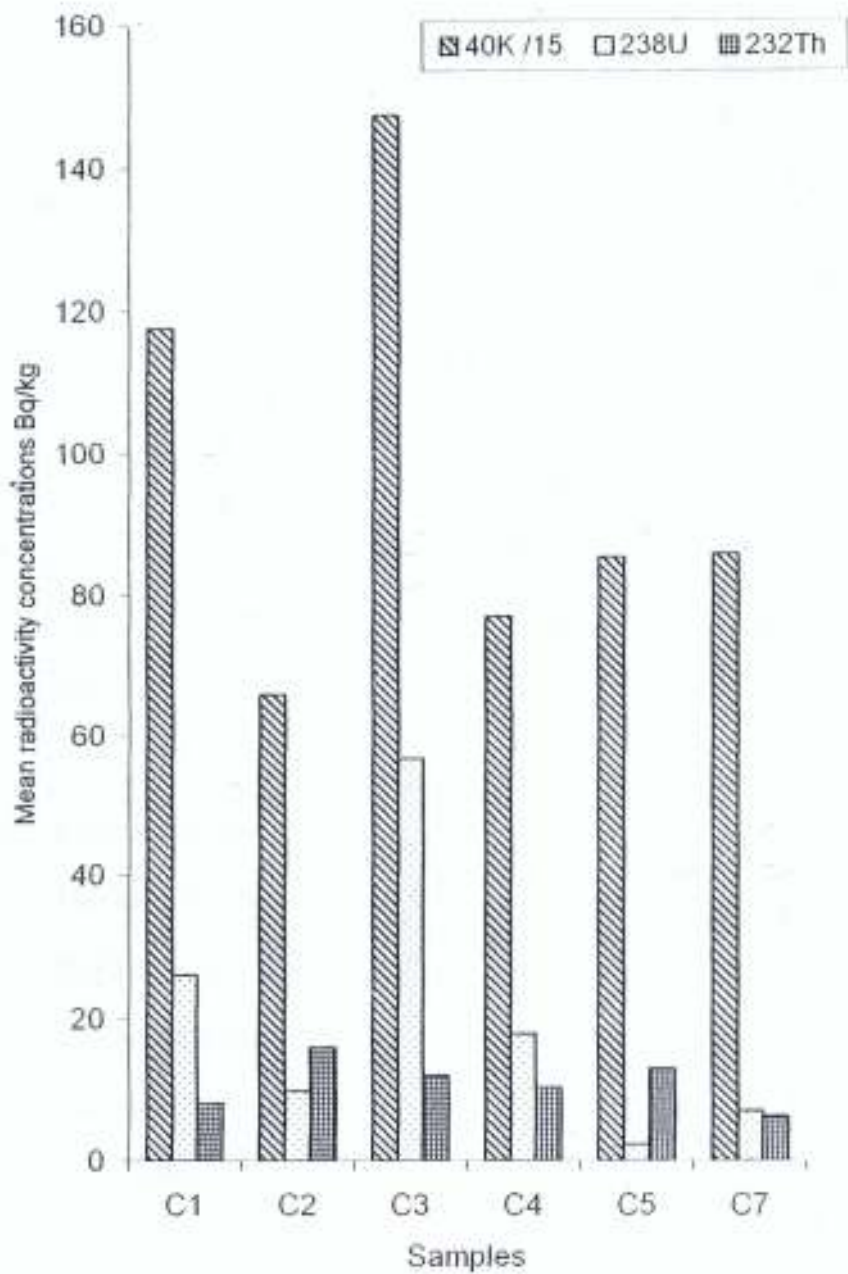


Fig. 5. 3 Mean radioactivity concentrations of ^{40}K , ^{238}U and ^{232}Th in location 3 (Agbabu)

Table 5.3 Mean radioactivity concentrations of the radionuclides in location 3

| Sample | ^{40}K (Bqkg $^{-1}$) | ^{238}U (Bqkg $^{-1}$) | ^{232}Th (Bqkg $^{-1}$) |
|----------------|---------------------------------|----------------------------------|-----------------------------------|
| C ₁ | 1764.79 ± 113.54 | 26.09 ± 4.41 | 8.23 ± 2.18 |
| C ₂ | 986.32 ± 50.73 | 9.88 ± 1.97 | 15.99 ± 3.32 |
| C ₃ | 2208.69 ± 65.60 | 56.65 ± 2.83 | 12.04 ± 1.27 |
| C ₄ | 1153.14 ± 56.57 | 17.99 ± 3.04 | 10.32 ± 1.36 |
| C ₅ | 1278.90 ± 68.34 | 2.36 ± 0.34 | 13.06 ± 2.73 |
| C ₇ | 1286.49 ± 38.81 | 7.06 ± 1.31 | 6.23 ± 0.76 |

C₁= *Amaranthus spp*

C₂= *Telfairia Occidentalis*

C₃= *Talium Triangulare*

C₄= *Venonia amygdahna*

C₅= *Solanum macncarpon*

C₇= *Corchorous Oltortus*

5.2 RELATIVE VARIATION OF RADIONUCLIDES CONCENTRATION ACROSS THE SPECIES

Figures 5.1- 5.3 and Tables 5.1- 5.3 indicate that the highest and lowest ^{40}K concentration were consistently found in Gbure (*Talium Triangulare*) and Ugwu (*Telfairia Occidentalis*) respectively at all the locations of study. While the highest and lowest concentrations of the others, ^{238}U and ^{232}Th , vary across the locations.

Obviously ^{40}K have the highest concentration in all the species. The high concentration of ^{40}K obtained for all the vegetables is due to its natural abundance in the soil and the use of potassium rich fertilizer. $^{232}\text{Th} / ^{238}\text{U}$ ratios for all the vegetables are less than unity as the concentrations of ^{238}U is always greater than that of ^{232}Th in all the species. The concentration of ^{238}U and ^{232}Th are generally low. This could be attributed to differences in their radiochemistry. ^{238}U has two oxidation states and could easily form complexes with water their enhancing its solubility, which ease its absorption by the root system. On the other hand, ^{232}Th has only one oxidation state and does not readily form complexes with water; has very low solubility and hence poor absorption by the root system.

Therefore the higher ^{238}U concentration at the leaves compared with the lower values of ^{232}Th concentration, can be explained in terms of the radiochemistry, absorption and upward transportation of nutrients to the plants leaf foliage. These factors combined to determine the availability of the radionuclides at the leaves. An important assertion is that the less-than-unity ratio of $^{232}\text{Th} / ^{238}\text{U}$ is a reflection of the resultant effect of the dynamics of reaction between the mentioned radiochemistry solubility and upward transportation of the nuclides by capillarity effect.

5.3 SPATIAL DISTRIBUTION OF RADIONUCLIDES IN THE WINDOW OF STUDY

In attempt to investigate the variation in the radionuclides concentration across the stations of study, weighted mean values are used in drawing the bar charts indicating the variation of ^{40}K , ^{238}U and ^{232}Th as displayed in figures 5.4, 5.5 and 5.6. The concentrations of ^{40}K , ^{238}U and ^{232}Th are observed to be greatest at Idanre compare with other stations. Idanre is noted for its rocky landscape and igneous rocks are primary sources of the primordial radionuclides (<http://www.umich.edu/radinfo/>).

The concentration of ^{40}K at Agbabu is greater than that of Jegele, while the concentrations of ^{238}U and ^{232}Th at Jegele are greater than those at Agbabu. However the differences in the mean values of the same radionuclides at the two different stations are insignificant.

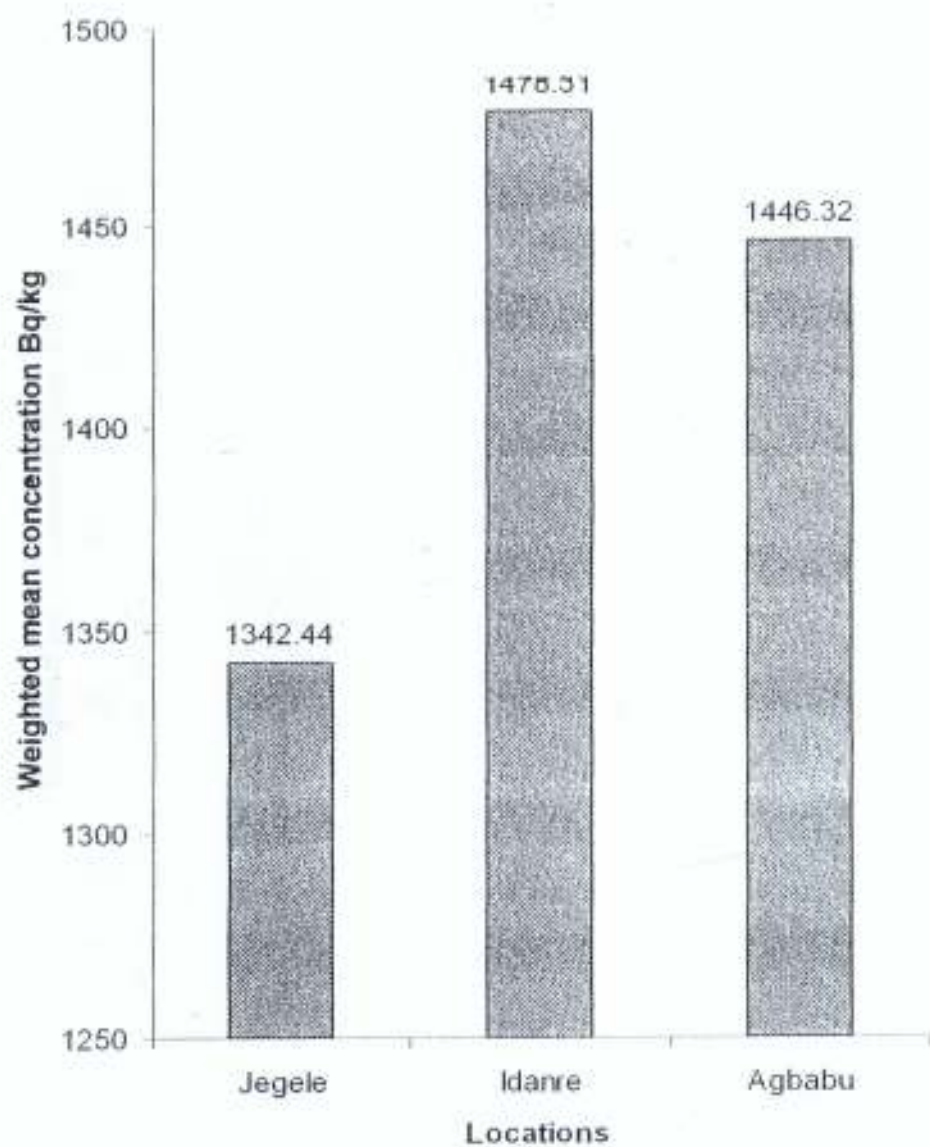


Fig. 5.4. Spatial Distribution of the ^{40}K Across the Three Stations

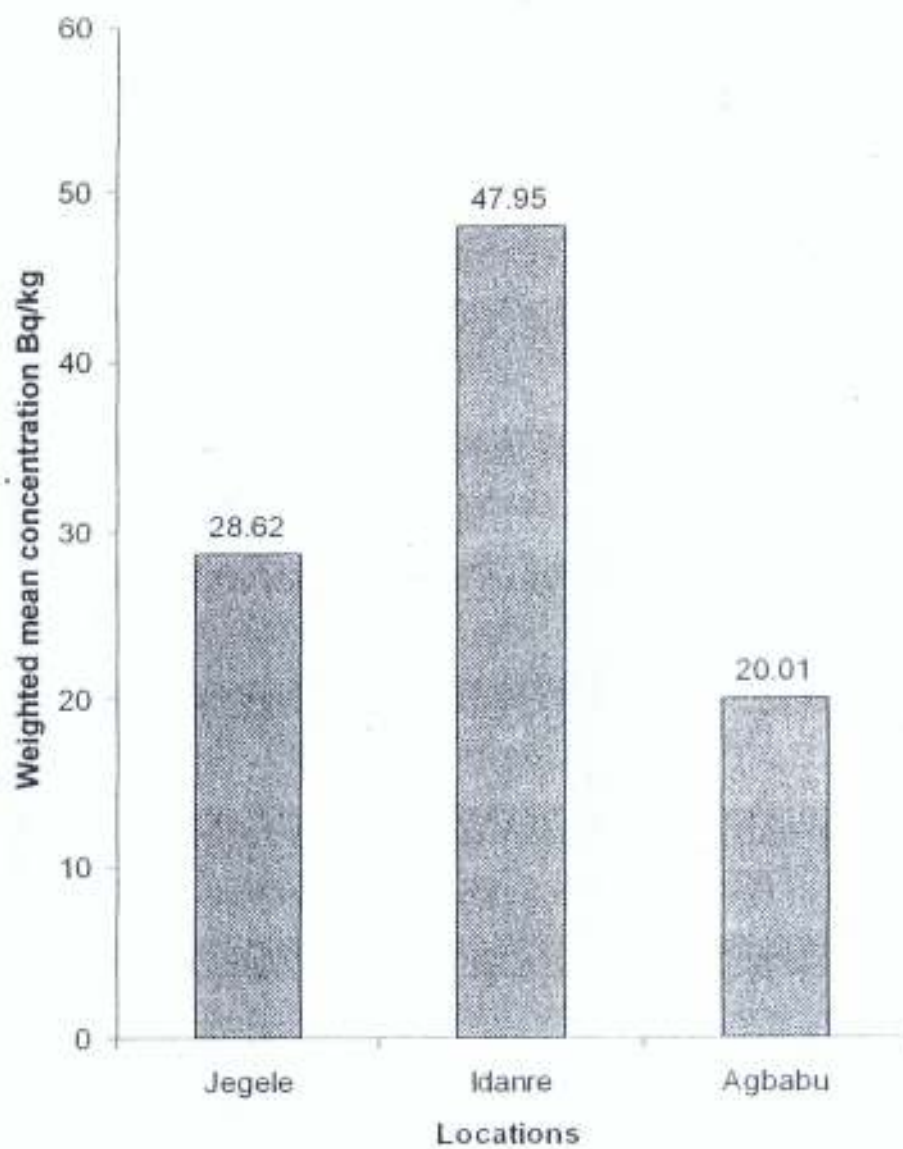


Fig. 5.5 Spatial Distribution of the ^{238}U Across the Three Stations

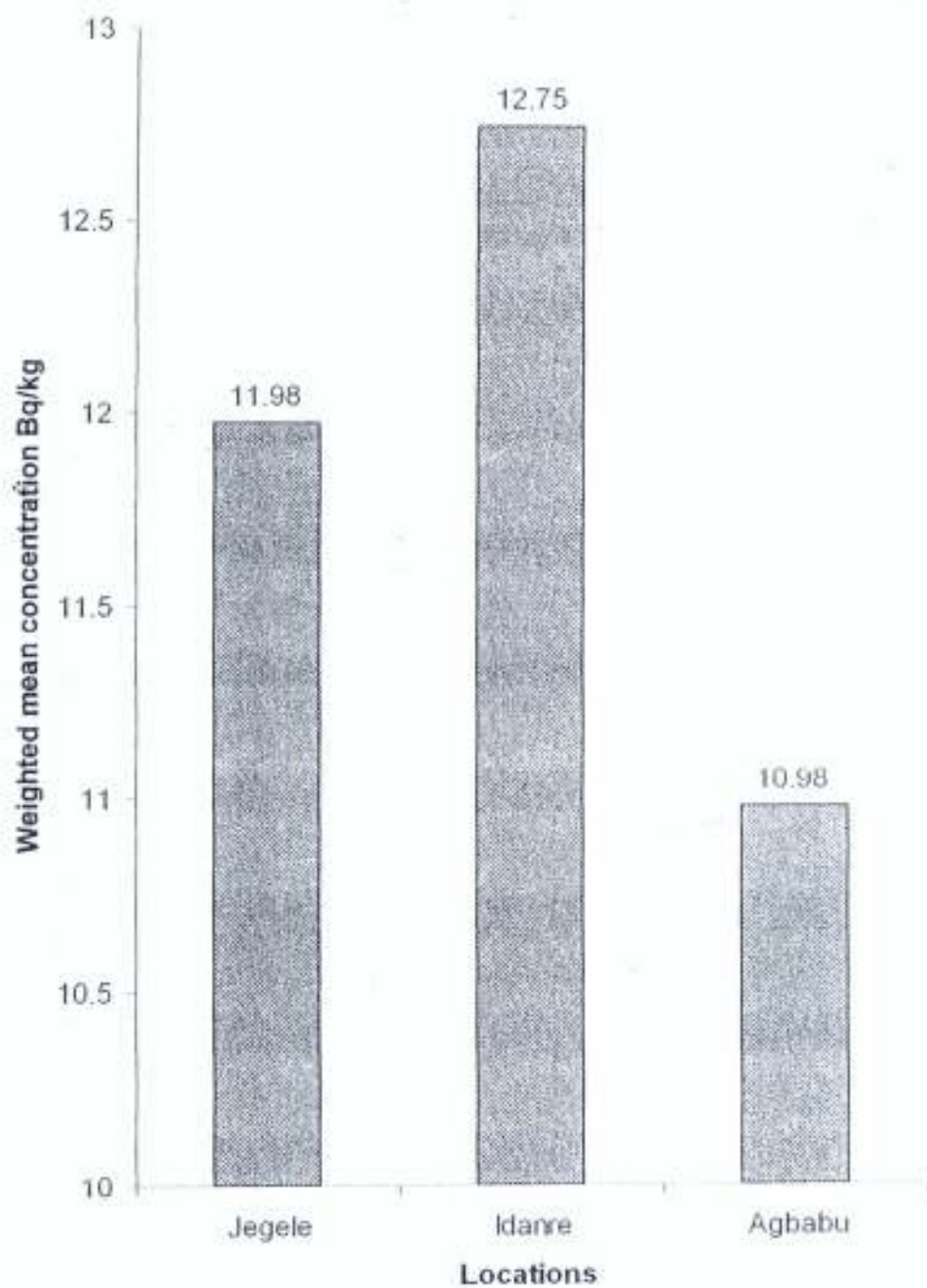


Fig. 5.6. Spatial Distribution of the ^{232}Th Across the Three Stations

5.4 EFFECTIVE DOSE EQUIVALENT AND COLLECTIVE EFFECTIVE DOSE EQUIVALENT

Radiation emitted by a radioactive substance is absorbed by any material it encounters. Every kilogram of material absorbs some energy. The amount of energy absorbed per kilogram of material is called the absorbed dose. It is measured in J/kg, which is called Gray (Gy) in radiation protection; it is expressed as a rate, which is Gyhr^{-1} (UIC, 2002). The doses received by a person consuming aquatic foodstuffs were reported by (Dougherty, 1988; Pentreath, 1988 and Akinloye et al 1999) which they found to be dependent on the radionuclides concentration of the food and the quantity taken. The effective dose incurred from a single radionuclide by an individual consuming a foodstuff is given by (Badran et al 2003) :

$$H_{ef} = G_r C_{rf} U_v \quad 5.1$$

where,

H_{ef} - effective dose equivalent by ingestion of nuclide (Sv/y)

G_r - dose conversion factor by ingestion of nuclide r (Sv/Bq)

C_{rf} = activity concentration of nuclide r in ingested food (Bq/kg)

U_v = consumption of vegetable (kg/y)

The dose calculations were based on the assumptions that each person obtained food according to the consumption defined in the food balance sheets for average adult per year 141.8Kg/y (FAO,2000) and radionuclide dose conversion factors for ^{40}K , ^{238}U and ^{232}Th are 5×10^{-9} , 4.6×10^{-8} and 2.3×10^{-7} Sv/Bq respectively for adults (ICRP,1994)

The effective dose from various radionuclides ingested in different vegetables was obtained by summing up over all nuclides. These are presented in Tables 5.4 – 5.6. The annual collective effective dose equivalent in the locations were obtained using ICRP expression

S_e - collective effective dose equivalent

H_i = average annual effective dose equivalent

$N(H)_i$ = number of individuals in the population sub group in the area.

Using equation 4.4 the effective dose equivalent for location 1 range between 0.41mSvyr^{-1} and 0.96mSvyr^{-1} , for location 2 the effective dose equivalent range between ND and 1.13mSvyr^{-1} . Lastly in the third location the effective dose equivalent ranges between 0.49mSvyr^{-1} and 0.98mSvyr^{-1} . Likewise using equation 5.2 this translates to a collective dose equivalent of $2.95 \times 10^2 \text{manSvyr}^{-1}$ for Akure when population figure of 499,999 (Encarta, 2000) was used, for Idanre it was $1.46 \times 10^1 \text{manSvyr}^{-1}$ when population figure of 19,999 (Encarta, 2000) was used, while $1.28 \times 10^1 \text{manSvyr}^{-1}$ was obtained for Agbabu with population figure of 19,999 (Encarta, 2000). These values are within the normal limit set by the International Commission on Radiological Protection (ICRP) (UIC, 2002) shown in Table 5.7. Table 5.7 reveals that effective dose which is below 2mSvyr^{-1} are for normal background. The effective dose equivalent from these three locations are below the recommended acceptable risk levels for health problem associated with radioactivity, although, the equivalent doses may increase with the exploitation of bitumen which is yet to start in location 3 due to disturbance of the natural equilibrium in course of exploitation.

Table 5.4 Effective Dose Equivalent in Location 1 Vegetables

| Sample | ^{40}K | ^{238}U | ^{232}Th | Effective dose Equivalent (mSvyr^{-1}) |
|----------------|-----------------|------------------|-------------------|---|
| C ₁ | 1725.28 | 27.96 | 12.34 | 0.76 |
| C ₂ | 721.6 | 28.94 | 8.54 | 0.41 |
| C ₃ | 2376.91 | 32.93 | 11.71 | 0.96 |
| C ₄ | 893.75 | 8.56 | 14.48 | 0.49 |
| C ₅ | 779.54 | 51.94 | - | 0.37 |
| C ₆ | 1613.63 | 47.66 | - | 0.61 |
| C ₇ | 1287 | 2.38 | 12.83 | 0.57 |

Table 5.5 Effective Dose Equivalent in Location 2 Vegetables

| Sample | ^{40}K | ^{238}U | ^{232}Th | Effective dose Equivalent (mSvyr^{-1}) |
|----------------|-----------------|------------------|-------------------|---|
| C ₁ | 1075.07 | 42.46 | 14.34 | 0.63 |
| C ₂ | ND | ND | ND | - |
| C ₃ | 2459.73 | 97.57 | 9.85 | 1.13 |
| C ₄ | 1169.16 | 25.01 | 8.38 | 0.53 |
| C ₆ | 1209.28 | 26.75 | 18.44 | 0.63 |

Table 5.6 Effective Dose Equivalent in Location 3 Vegetables

| Sample | ^{40}K | ^{238}U | ^{232}Th | Effective dose Equivalent (mSvyr^{-1}) |
|----------------|-----------------|------------------|-------------------|---|
| C ₁ | 1764.79 | 26.09 | 8.23 | 0.71 |
| C ₂ | 986.32 | 9.88 | 15.99 | 0.54 |
| C ₃ | 2208.69 | 56.65 | 12.04 | 0.98 |
| C ₄ | 1153.14 | 17.99 | 10.32 | 0.54 |
| C ₅ | 1278.9 | 2.36 | 13.06 | 0.57 |
| C ₇ | 1286.49 | 7.06 | 6.23 | 0.49 |

Table 5.7 Dose limits and their Biological Effects (After UIC, 2002)

| Radiation dose Rate | Duration of Exposure | Likely Effects/Implication |
|-----------------------------|----------------------|--|
| 10,000mSv | Short-term dose | Immediate illness and subsequent death with few weeks |
| 1,000mSv | Short-term dose | Nausea and decreased white blood cell, but not death |
| 50mSvyr ⁻¹ | Over 5 years | The lowest dose rates where there is any evidence of cancer being caused. Above this, the probability of cancer occurrence increases with dose |
| 2mSvyr ⁻¹ | | Normal background to all human on earth |
| 0.3-0.6 mSvyr ⁻¹ | | Artificial sources of radiation, mostly medical equipment |

5.5 CONCLUSION

The method of gamma spectrometry has been used to determine the radioactivity concentrations of seven (7) vegetable species from 3 locations in Ondo State Southwestern Nigeria. The results of the measurement showed that ^{40}K have the highest concentration in all the tested samples. Highest concentration of ^{40}K (2459.73Bqkg^{-1}) was obtained in Gbure (*Talium Triangulare*) in Idanre, the highest concentration of ^{238}U (97.57Bqkg^{-1}) obtained Gbure (*Talium Triangulare*) from Idanre, while the highest concentration of ^{232}Th (18.44Bqkg^{-1}) obtained in Rorowo (*African Spinach*), also from Idanre. Concentration of ^{40}K is high in the tested vegetable samples because potassium concentrates in leaves more than any other parts of plant and for this analysis the edible parts i.e. the leaves were used. Also due to increased used of potassium rich fertilizer. Results also indicate that the highest and lowest ^{40}K concentrations were consistently found in Gbure (*Talium Triangulare*) and Ugwu (*Telfairia Occidentalis*) respectively at all the locations of study. While the highest and lowest concentrations of the others, ^{238}U and ^{232}Th , vary across the locations.

Idanre was found to have highest concentrations ^{40}K , ^{238}U and ^{232}Th , this confirms that igneous rocks are the primary source of the primordial radionuclides, since Idanre is a town of full and surrounded by rocks. The lowest concentration of ^{40}K (721.86Bqkg^{-1}) was found in Ugwu (*Telfairia Occidentalis*) in Akure; ^{238}U (2.36Bqkg^{-1}) was obtained in Igbo (*Solanum Macncarpon*) in Agbabu, while ^{232}Th (6.23Bqkg^{-1}) found in Ewedu (*Corchorous Olitorious*) also in Agbabu.

$^{232}\text{Th} / ^{238}\text{U}$ ratios for all the vegetables are less than unity as the concentrations of ^{238}U is always greater that that of ^{232}Th in all the species. The higher ^{238}U concentration at the leaves compared with the lower values of ^{232}Th concentration, can be explained in terms

of the radiochemistry, absorption and upward transportation of nutrients to the plants leaf foliage.

The radioactivity concentrations have been used to determine the effective dose equivalent due to the three primordial radionuclides in the vegetables and consequently the collective effective dose equivalent. The average dose rate for Akure, Idanre and Agbabu were found to be 0.59mSvyr^{-1} , 0.73mSvyr^{-1} and 0.64mSvyr^{-1} . The highest effective dose equivalent rate of 1.13mSvyr^{-1} was obtained in Gbure (*Talium Triangulare*) in Idanre, while the lowest dose equivalent of 0.41mSvyr^{-1} was obtained in Ugwu (*Telfairia Occidentalis*) in Akure. These translate to collective doses of $2.95 \times 10^2 \text{manSvyr}^{-1}$, $1.46 \times 10^1 \text{manSvyr}^{-1}$, and $1.28 \times 10^1 \text{manSvyr}^{-1}$ for Akure, Idanre and Agbabu respectively. These values are lower than the 2mSvyr^{-1} for normal background (UIC, 2002), which shows that the consumption of the investigated vegetables does not convey any risk to the health of the population in the considered locations. The effective dose equivalent may increase with the exploitation of the bitumen due to the disturbance of the natural equilibrium since is yet to commence.

5.6 LIMITATIONS AND SUGGESTION FOR FURTHER STUDIES

This is a pioneering study of the radioactivity in vegetables commonly consumed in Ondo State most especially in Agbabu where bitumen has been discovered. The study has achieved its objective within the limits of available resources. Number of samples and towns were small due to limited financial resources and dry season. The results for limited samples considered are generalized for the town. In further study more samples from different farms in the towns can be analyzed to avoid error due to generalization and to build on the results.

- Agu, B.N. (1965).** Observation of radioactive fallout in Nigeria up to 1961. *Nature*, **205**, 649-651.
- Ajayi, O.S. (2000).** Environmental gamma radiation indoors at Akure, southwestern Nigeria. *J.Sci. Engr. Tech*, **6** (2), 1660-1667
- Ajayi I.R, Oresegun M.O and Babalola I.A. (1996).** Absorbed dose rates in air due to U, Th and K in a part of Southwestern Nigeria. *Nig. J. Phys.*, **8**, 38 – 40.
- Ajayi, I.R. and Asubiojo, O.I. (1983).** Distribution of rare element in granite gneisses from Ife-Ilesa schist belt. *Nig Jour. Sci.*, **17**, 111 – 123.
- Akinloye, M.K., Olomo, J.B. and Olubunmi, P.A. (1991).** Meat and Poultry consumption contribution to the natural radionuclides intake of the inhabitants of the Obafemi Awolowo Univ., Ile-Ife, Nigeria. *Nucl. Instru. and meth.*, **A422**, 795-800
- Arogunjo, A.M.; Farai, I.P. (1999).** Radiological implication of gamma radiation level in southwestern Nigeria. *J.Sci. Engr.*, **6** (2), 1660-1667
- Arogunjo, A.M. (2002).** Measurement of radioactivity level in the oil producing areas in the Delta region of Nigeria. PhD thesis, Federal University of Technology, Akure
- Arogunjo, A.M. (2003).** Natural radionuclides content of some local cereals in Akure, southwestern Nigeria. *Nig. J. of pure and applied Phys.*, **2** (1), 34-35
- Babalola I.A. (1984).** Radiation measurement and assay of tailings from high natural radioactivity in Jos Plateau State. *Nig. J. Sci.*, **18**, 98 – 101
- Badram H.M., Sharshar T and Elmimer (2003).** Levels of ^{137}Cs and ^{40}K in edible parts of some vegetables consumed in Egypt. *Jour. of Environment Radioactivity*, **67**, 181 - 190
- Beck, H.L., De campo and Gologat, J. (1972).** 'In - situ Ge - Li and NAI (TI) gamma ray spectrometry' HASL - 258
- BEIR V (NAS).** <http://www.nap.edu/catalog/1224.html>

- Ben-nai, I. ; Yoshida, S.; Muramatsu, Y (1994).** Cultivation experiment of uptake of radionuclides by mushroom. *Radioisotopes* **43**: 77-82; (in Japanese)
- Birks, J. P. (1964).** Theory of Scintillation Counting, Pergamon Press, London.
- Delaune, R.D.; Jones, G.L.; Smith, C.J. (1986).** Radionuclide concentrations in Louisiana soils and sediments. *Health Physics* **57**:239-244
- Dougherty, G. (1988).** Environmental radioactivity concentration levels in marine species from Malaysia and Fiji *Health Phys.*, **57** (1), 187-190
- Eisenbud, M. (1987).** Environmental radioactivity from natural, industrial and military sources. Academic press, Inc. Harcourt Brace Jovanovich publishers. New York.
- Farai, I.P. (1989).** ^{222}Rn survey in groundwater and its assessment for radiological hazards and seismic monitoring in Nigeria. PhD thesis, University of Ibadan.
- Farai, I.P. and Sanni, A.O. (1992a).** Year long variable of ^{222}Rn in a ground water system in Nigeria. *J. of African Earth Sci.*, **15**, 399-403
- Farai, I.P. and Sanni, A.O. (1992b).** ^{222}Ra in a groundwater in Nigeria: A survey. *Health Physics*, **62** 96-98
- Farai I.P. and Jibri N.N. (2000).** Baseline studies of terrestrial outdoor gamma dose rate levels in Nigeria *Radiation Protection Dosimetry* **88** (3), 247 - 254
- Farai I.P. and Oni O.M. (2002).** Natural radionuclide concentrations in aquatic species and absorbed dose equivalents to the dwellers of the coastal areas of Nigeria *Nig. Jour. of Phy.*, **14**, 94 - 97
- Feldman, K.L. (1977).** Radiological quality of the environment in the United States. Washinton DC. U.S. Environmental Protection Agency, EPA 520/1-77-009
- Fortunati, P.; Brambilla, M.; Speroni, F. and Carini, F. (2004).** Foliar uptake of ^{134}Cs and ^{85}Sr in strawberry as function by leaf age *J. of Environmental Radioactivity* **71**, 187-199
- IAEA (1989).** Technical report series, **295**

ICRP (1994). Recommendations of the International Commission on Radiological Protection Pergamos Press

Jibri, N.N. and Farai, I.p.(1998). Assessment of dose and collective effective dose equivalent due to terrestrial gamma radiation in the city of Lagos, Nigeria. *Rad protect Dosim.* 76 (3),191-194

<http://www.cord.org/step-online>

<http://www.umich.edu/radinfo/>

<http://www.fao.org/WAICENT/INFO/>

Komamura, m.; Yuita, K.; Yamazaki, S.(1994). Radiation research of soil and grain of rice and wheat . in proceedings of the result of study on environment radiation research Tokyo: Science and Technology Agency: 15-16; (in Japanese).

Knoll G.F. (1989). 'Radiation protection and measurement' 2nd edition, John Wiley and Sons, New York.

Microsoft Encarta Encyclopedia (2000).

National Council on Radiation Protection and Measurements (1987). Reports 64, 94, 95, 103 and 116, Washington DC

National Radiological Protection Board (1989). Living with radiation (NRPB)

Olomo, J.B.,(1990). Natural radionuclide content of some Nigeria food stuffs. *Nucl. Inst. and methods in Phys. Res.*, A 299,666-669.

Olomo J.B, Akinloye M.K. and Balogun F.A (1994). Distribution of gamma emitting natural radionuclides in soils and water around nuclear research establishments, Ile – Ife, Nigeria' *Nucl. Instrument methods*, A 353, 553 – 557

Ondo State website. www.ondostategovernment.com

Oresegun, M.O. and Babalola, I.A. (1990). 'Occupational radiation Exposure associated with milling of Th –U RICH Sn in Nigeria' *Health Physics*, 58, 213-215

- Pentreath, B.J. (1988).** Radionuclides in the food chain M.W. Carter (ed.), Springer Verlag, New York, 108-109
- Sprawls, P. (1995)** Physical principles of medical imaging, Medical physics Publishing House Saunders
- Thompson, I.M.G.; Botter-Jensen, L.; Deme, S.; Pernicka, F. and Saez-Vergara, J.C. (1999).** Technical recommendations on measurements of external environmental Uranium Information Centre (2002). Radiation and Life U.I.C.
<http://www.uic.com.au/ral.htm>
- UNSCEAR, (1993).** Ionizing radiation: Sources and biological effects, United Nation Scientific Committee on the Effects of Atomic Radiation Report
- Yu, K.N.; Guan, Z.J.; Young, E.C.M.; Strokes, M.J. (1993).** In-situ measurements of radon exhalation rate from building surface in Hong Kong. *Nucl. Sc. Techniques*, **4**, 176-180
- Yu, K.N.; Young, E.C.M.; Li, K.C. (1996).** A survey of radon properties for dwellings for Hong Kong. *Rad. Protect. Dosim.*, **63**, s 55-62